

**The Climate of the Eocene-Oligocene-Transition
during the Antarctic Ice Sheet Buildup:
Modern Climate Model Simulations**

Masterthesis



Universität Bremen, Fachbereich 1

by

Hanna Sophie Knahl

Examiners & Supervisors

Prof. Dr. Gerrit Lohmann

Dr. Johann Klages

Technical Supervisor

Paul Gierz



Alfred-Wegener-Institut

The Climate of the Eocene-Oligocene-Transition during the Antarctic Ice Sheet Buildup: Modern Climate Model Simulations

Masterthesis



Universität Bremen, Fachbereich 1

by

Hanna Sophie Knahl

Examiners & Supervisors

Prof. Dr. Gerrit Lohmann

Dr. Johann Klages

Technical Supervisor

Paul Gierz

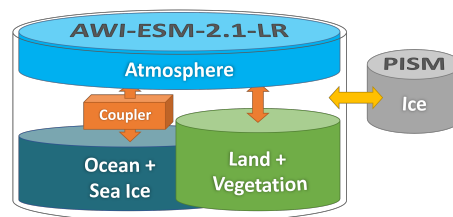


Alfred-Wegener-Institut

Bremen, 1st of December 2022

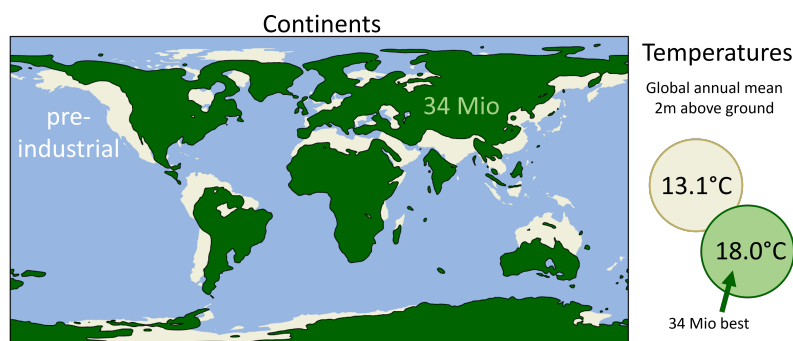
0. Public Summary

Paleoclimate science travels back in time of earth's climate history. There are two "time travelling" methods: running a computer model or reading in climate archives. In this thesis I use a climate model simulating the climate 34 Million years ago. Afterwards, I compare my results to data from climate archives. I choose the time 34 Million years ago because this was a fascinating time full of change. It was a transition between two geological epochs: from the Eocene to the Oligocene. In the warm Eocene Antarctica was not covered by ice. Earth was in a so called "Greenhouse" climate. During the Eocene-Oligocene-Transition the climate cooled down to an "Icehouse" climate and the Antarctic ice sheet began to build up. Since this happened far back in time, there are still uncertainties about the climate and the development of the ice sheet. This thesis helps to get a better idea on that.



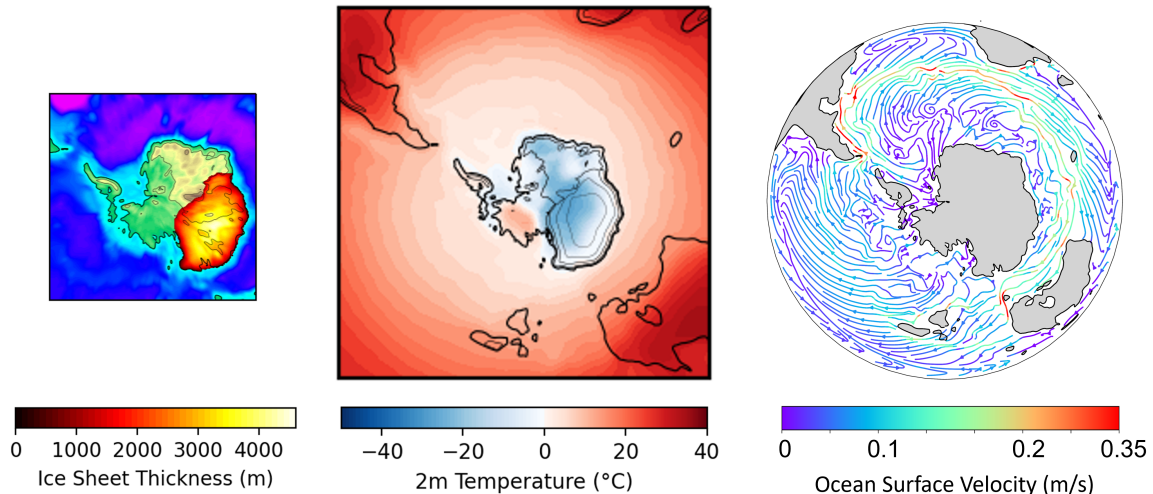
The schematic set up of the used climate and ice model

For the climate simulations I use the modern global Earth System Model AWI-ESM-2.1. It couples models for ocean, atmosphere and land surface. So, all these dynamic earth system components work hand in hand. The Antarctic ice sheet is modelled by my colleague Lu Niu using an ice model. The boundary conditions for the models, like the position of the continents, are based on reconstructions and assumptions. During



Continents and temperatures 34 Mio years ago (green) and pre-industrial (white).

the Eocene-Oligocene-Transition it was probably warmer than in pre-industrial times (approx. 150 years ago). The model indicates 0.4°C to even 4.9°C more. Where comes this range from? I test different CO₂ levels for the paleo model runs as the exact CO₂ concentration in the atmosphere is uncertain for that time. And, as we learn from the present climate change, higher CO₂ levels cause higher temperatures. The figure *Ice Sheet*



(left) Possible Antarctic ice sheet, (middle) according summer air temperatures 2m above the ground, (right) ocean currents

Thickness shows how the Antarctic ice sheet could have looked like 34 Million years ago. The East is covered by ice up to 4,500m thick. In the West the model did not develop any ice. There it is generally too warm. Air temperatures in the West Antarctic lie around 0 – 10°C in the Antarctic summer. Above the ice sheet summer temperatures are much lower and reach down to –20°C. The model also indicates only very few sea ice in summer in the Antarctic. These results support findings from a sediment core, a climate archive. The sediment core was drilled near the West-Antarctic coast and shows no signs of a big ice sheet or sea ice close to the drill site. The ocean currents show an interesting pattern, too. Around the pole an Eastward current develops and weak gyres form in the large Antarctic bays. This means part of the heat from the equator can be transported to Antarctica and parts are "caught" in the circumpolar current. The results from the sediment core together with climate model results from this Master thesis are published in the paper (Klages et al., under review) (for details see References (section 7)).

1. Abstract

The Eocene-Oligocene-Transition (EOT) marks the significant change from a "Greenhouse" to an "Icehouse" climate during the Cenozoic (Bohaty et al., 2012). This work presents modelled climate conditions during the EOT and contributes to the discussion about Antarctic glaciation. The strength of this work lies in the use of a modern fully-coupled Earth System Model (ESM), the high resolution applied to the polar regions and the strong comparison to proxy data. The model results combined with new West Antarctic proxy data from Klages et al., under review strongly support the hypothesis of an asymmetric Antarctic Ice Sheet (AIS) and West Antarctic deciduous forest vegetation. Observed CO₂ thresholds for Antarctic glaciation are > 840 ppm for the onset of glaciation and < 560 ppm for a continental-scale ice sheet reaching into West Antarctica. For the Southern ocean heat transport an intermediate state between a subpolar gyre and an Antarctic Circumpolar Current (ACC) regime is modelled. West Antarctic temperatures are several degrees lower compared to proxy data but agree with other modelled temperatures. Summer air temperatures are between -5 – 5°C. Summer sea surface temperature (SST) ranges within -1 – 5°C and allow only few summer sea ice. The modelled EOT climate is several degrees warmer than the pre-industrial (PI) climate on all latitudes. The global annual mean air temperature lies almost 5°C above the reference PI simulation. With 18.0°C it is relatively low compared to other modelled temperatures. Global vegetation known from proxy data can partly be resolved by the model. Overall, this model supports an ice free West Antarctic during the EOT found in Klages et al., under review and provides a detailed framework for Antarctic ice in global EOT climate dynamics. The largely good agreement with EOT proxy data encourages deep time modelling with AWI-ESM-2.1.

Contents

0. Public Summary	1
1. Abstract	3
2. Introduction	10
3. Methods	13
3.1. The Model AWI-ESM-2.1-LR	13
FESOM2.1	13
ECHAM 6.3.05p2	14
JSBACH	15
OASIS3 coupler and ESM-tools	15
3.2. Topography and Bathymetry	16
3.3. Model Runs	17
4. Results	20
4.1. Antarctic Climate in the EOT Model	20
4.1.1. Antarctic Ice	20
4.1.2. Antarctic Temperatures	22
4.1.3. Ocean Currents and Precipitation	26
4.2. Global Climate in the EOT Model	27
4.2.1. Global Temperatures	27
4.2.2. Global Vegetation	33
5. Discussion	34
5.1. Antarctic Climate and Ice Sheet	34
5.1.1. Reasonable Atmospheric CO ₂ Concentrations	34
5.1.2. Comparison to Antarctic Climate in Drill Cores	35
5.1.3. Comparison to other Glaciation Modelling Results	38
5.1.4. The Impact of Gateways	40
5.2. Global Climate	41
5.2.1. Temperature Comparison to Proxy data and different models	41

5.2.2. Global Vegetation Comparison to Proxy Data	43
6. Conclusion	46
7. Recommendations	48
Acknowledgments	51
References	52
A. Technical Details	57
Declaration	58

List of Figures

1.	The model set up used for the simulations. The AWI-ESM-2.1-LR model manually coupled with the PISM ice model for the AIS.	13
2.	(left) FESOM mesh horizontal resolution. The mesh is unstructured and prismatic. Note that the resolution is highest at the poles as the Southern polar region is the region of highest interest. (right) ECHAM6 T36 grid resolution. Adapted from Sidorenko et al., 2015	14
3.	The reconstructed Bathymetry and Topography for the Eocene-Oligocene-Transition used for the model simulations	16
4.	The topography and bathymetry in the region of three important gateways: (left) Drake passage, (centre) Tasmanian gateway, (right) Atlantic Arctic oceanic gateway. (Top) Map of the region, (bottom) cross section within the narrowest and flattest part	17
5.	Order of the model runs including the PISM runs performed by Lu Niu .	19
6.	Quasi-equilibrium of the atmospheric model (top) exemplary shown for global annual mean 2m temperature (left) and sea surface temperature (right). The deep ocean has not yet reached the quasi-equilibrium, exemplary shown by the salinity in 1000 m of depth (bottom). All figures show 250 model years for the climate without and with Antarctic ice sheet with a CO ₂ level of 3x PI.	19
7.	(left) Antarctic ice sheets from PISM runs with climate under the three different CO ₂ levels. (right) Summer Antarctic sea ice of the EOTice runs.	21
8.	February mean 2m air temperatures over the Antarctic region	24
9.	February mean water surface temperatures in the Southern ocean	25
10.	Streamplot of the ocean surface velocity	26
11.	Annual total precipitation in the Antarctic region (large scale precipitation + convective precipitation)	27
12.	2m air temperature and water surface temperature global annual means over the last 50 model years	28
13.	50-year annual zonal mean 2m temperature and water surface temperatures for all model runs	30

14.	50-year annual mean 2m air temperatures for all model runs	31
15.	50-year annual mean water surface temperatures for all model runs	32
16.	Maximal vegetation fraction per grid cell of the EOT3ice run. Red represents the extend of the ice sheet. White can also indicate no vegetation coverage like in the Antarctic.	33
17.	Approximate paleo-location of the sediment core (site PS104-21) in the Amundsen Sea (red star) with paleolatitude $\sim 73.5^\circ S$ (Klages et al., under review) in the used EOT topography and bathymetry	36
18.	Difference in 2m air temperature between the ice and no-ice runs for 2x and 3x CO ₂ levels	43

List of Tables

1.	The here applied PFTs.	15
2.	Climate model runs by name, EOT of pre-industrial setup, CO ₂ concentration relative to the PI conditions (1× = 274.8 ppm, 2× = 560 ppm, 3× = 840 ppm), ice sheet covering Antarctica and modelled years which were used (modelled but not used)	18
3.	Annual mean temperatures at the location of the drill core (mean of four grid cells closest to drill location (see Figure 17)) for the EOTice and PI runs. The mean of the last 50 (*30) model years is taken	23
4.	Annual mean temperatures for the different model runs over the last 50 (*30) model years	27
5.	Comparison of modelled PFTs and vegetation proxy data. Proxy data for Antarctica are taken from (Klages et al., under review) and the global rest from (Pound and Salzmann, 2017).	45

List of Acronyms

ESM Earth System Model

EOT Eocene-Oligocene-Transition

PI pre-industrial

PFT plant functional type

AIS Antarctic Ice Sheet

WAIS West Antarctic Ice Sheet

EAIS East Antarctic Ice Sheet

ACC Antarctic Circumpolar Current

SST sea surface temperature

AMOC Atlantic Meridional Overturning Circulation

2. Introduction

The EOT ($\sim 34.4 - 33.7$ Ma) marks a significant climatic change within the Cenozoic era. During this transition the climate performed a shift from a "Greenhouse" to an "Icehouse" climate (Bohaty et al., 2012). Late Eocene atmospheric CO_2 levels were about 1000 ppm (Anagnostou et al., 2016) and dropped by several 100 ppm during the transition (Hutchinson et al., 2021; Pagani et al., 2011). Sea water $\delta^{18}\text{O}$ values increased during the EOT and indicate an increase in global ice volume up to a level of 60 – 130% modern East Antarctic Ice Sheet (EAIS) (Bohaty et al., 2012). So, major glaciation must have happened during the climate transition. Antarctica could have strongly contributed to the ice volume increase as already then it represented a large landmass in a polar region (Paxman et al., 2019) and glaciation coincided with high latitude cooling (Bohaty et al., 2012).

First evidence of an EAIS was found in sediment drill cores in Prydz Bay (Zachos et al., 1992). It supposes an ice volume comparable to present-day conditions around ~ 36 Ma. Proxy data from the Ross sea indicate a close by continental-scale ice sheet after 32.8 Ma (Galeotti et al., 2016). Contrastingly, new proxy data from West Antarctica show no signs for a continental scale ice sheet reaching into the West Antarctic during the EOT. The sediment drill core in the Amundsen sea indicates no grounded ice sheet, but vegetation instead, and therefore proposes a minor West Antarctic Ice Sheet (WAIS) (Klages et al., under review). These new data are the motivation for this work because they arise the question how and where glaciation proceeded during the EOT if only minor contribution can be expected from West Antarctica. Several model studies already modelled possible AIS for the EOT but lead to very different results (Jamieson et al., 2010; Wilson et al., 2013; DeConto et al., 2007; Van Breedam et al., 2022). This work tackles the question of Antarctic glaciation by modelling possible EOT climates and its influence on the AIS build-up.

The hypothesis for this study is that the climate allows an asymmetric AIS. A major ice volume is expected in the East Antarctic and only minor ice in the West Antarctic which should still be covered by vegetation similar to Patagonian biomes today (Klages et al., under review).

Climate and ice sheets are closely linked. Ice sheet growth is dependent on many regional climate components, such as temperature, precipitation and insolation. These local climate components are influenced by the global climate conditions. A growing ice sheet in reverse is influencing the regional albedo and the global oceanic thermohaline circulation (Wallace and Hobbs, 2006).

The strength of this work is that it uses the fully coupled ESM (AWI-ESM-2.1) with components for ocean, sea ice, atmosphere and land surface. This model is capable to deliver detailed and strong global climate information on high polar resolution. Combined with the ice sheet model PISM we expect strong indications on Antarctic climate conditions, such as ice sheets, temperatures, vegetation and ocean currents.

There are three different typical forcings applied to ESMs for studying the EOT climate: changes of atmospheric CO₂, the AIS or the paleogeography (Hutchinson et al., 2021). In this study we decided to keep the geography constant, while using three different CO₂ levels (1x, 2x and 3x PI CO₂) and observing the development of the according AISs. This decision is supported by the finding that the change of CO₂ concentration has a much larger effect on surface air temperatures than glaciation and geography changes (Hutchinson et al., 2021).

The AIS build up is only observed when atmospheric CO₂ falls below a certain threshold. Modelling and proxy studies propose different CO₂ thresholds for the Antarctic glaciation (DeConto and Pollard, 2003; Galeotti et al., 2016; Ladant et al., 2014). Modelled thresholds are found to be highly dependent on the model and model set up and can range between 560 – 920 ppm for intermediate glaciation (Gasson et al., 2014). The three CO₂ levels used in this work are chosen to picture the model's threshold behaviour and to cover uncertainties on the EOT CO₂ level (Hutchinson et al., 2021).

There still remain uncertainties in the reconstruction of the EOT paleogeography (Paxman et al., 2019; Hutchinson et al., 2021). The Southern gateways were opening around that time and are expected to play an important role in Southern ocean circulation and heat transport (Sauermilch et al., 2021; Scher et al., 2015). It is discussed whether the openings already allowed to develop the ACC, thermally isolating the Antarctic climate,

(Barker and Thomas, 2004) or if heat was still transported into the Antarctic via subpolar gyres (Sauermilch et al., 2021). But timing and deepening, especially of the Drake passage are still uncertain (Livermore et al., 2007). Also, there exist different reconstructions on global and in particular West Antarctic topography which is expected to have have an important influence on the development of the AIS (Hutchinson et al., 2021; Paxman et al., 2019).

Proxy data resolve EOT vegetation for most parts of the world (Pound and Salzmann, 2017, Klages et al., under review). Reconstructions from these biomes describe a global climate to be generally warmer than today (Pound and Salzmann, 2017). Different model simulations show global annual mean surface temperatures from 16.5 – 25°C for 2x PI CO₂ levels and even higher temperatures for higher CO₂ levels (Hutchinson et al., 2021). So, the comparison to the reference PI simulation is expected to show a generally warmer climate.

3. Methods

3.1. The Model AWI-ESM-2.1-LR

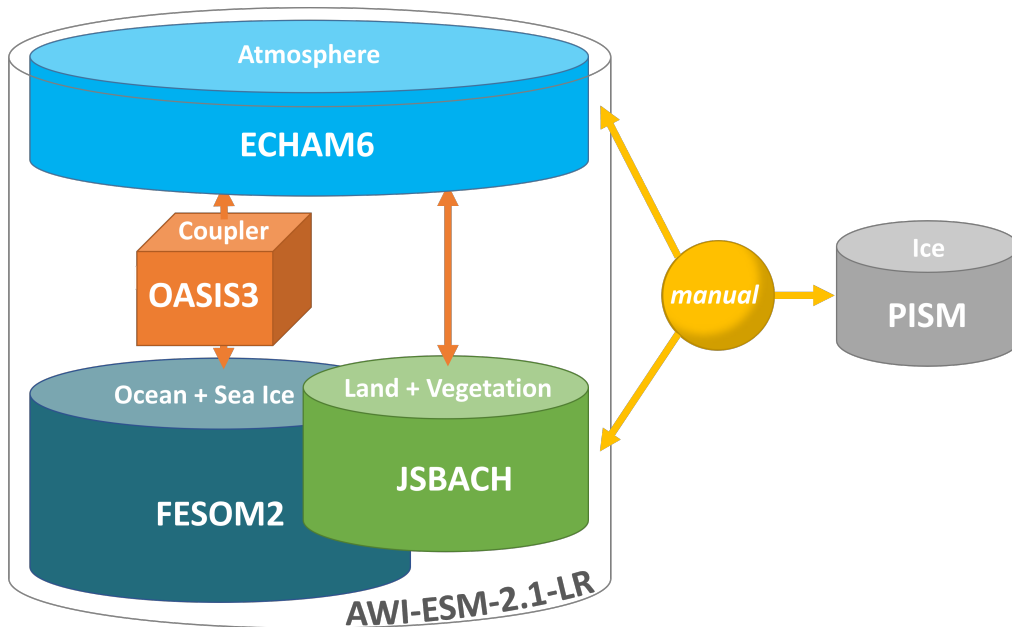


Figure 1: The model set up used for the simulations. The AWI-ESM-2.1-LR model manually coupled with the PISM ice model for the AIS.

For my thesis I used the state-of-the-art Alfred Wegener Institute Earth System Model version 2.1 (AWI-ESM-2.1-LR). The set up is shown in Figure 1. It contains the ocean model FESOM2 and the atmosphere model ECHAM6 which are coupled by the Oasis coupler. Land surface and vegetation is modelled by JSBACH which is directly coupled to the atmosphere model. The ice sheet model runs were performed with the Parallel Ice Sheet Model (PISM) by Lu Niu. It follows a short description of each model, their resolutions and the reconstructed data.

Ocean and Sea Ice by FESOM2.1

The Finite-volumE Sea ice Ocean Model FESOM2.1 is a modern global ocean model which was developed at the Alfred-Wegener-Institute (Danilov et al., 2017). It uses an unstructured prismatic high-resolution mesh. Due to the use of the finite-volume approach the computational efficiency of FESOM2.1 is comparable to state-of-the-art ocean models

with structured meshes (Scholz et al., 2019). The advantage of an unstructured mesh is its geometric flexibility (Koldunov et al., 2019). Furthermore, the resolution of FESOM2.1 is variable. The here used resolutions are CORE2 for the grid resolution shown in Figure 2 (left) and L46 for the vertical resolution. The grid resolution changes over latitudes are shown in Figure 2. The sea ice is modelled within FESOM2.1 by the included sea ice model Finite-Element Sea Ice Model (FESIM).

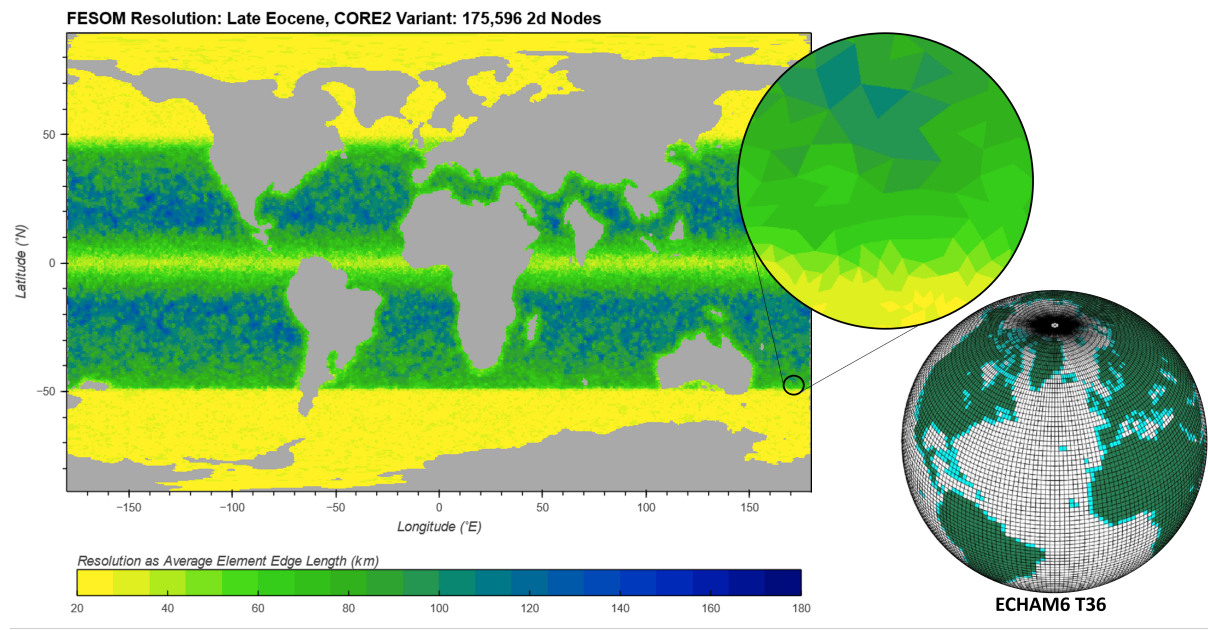


Figure 2: (left) FESOM mesh horizontal resolution. The mesh is unstructured and prismatic. Note that the resolution is highest at the poles as the Southern polar region is the region of highest interest. (right) ECHAM6 T36 grid resolution. Adapted from Sidorenko et al., 2015

Atmosphere by ECHAM 6.3.05p2

ECHAM6 is an atmospheric general circulation model. Here I used the version ECHAM 6.3.05p2. It couples diabatic processes and large-scale circulations (Stevens et al., 2013). The horizontal grid is resolved in T63 as shown in Figure 2 (right). The vertical resolution is L47 which resolves the atmosphere until 0.01 hPa in a hybrid sigma-pressure coordinate system applied on a Lorenz grid (Stevens et al., 2013).

Land surface and vegetation by JSBACH

The Joint Scheme for Biosphere Atmosphere Coupling in Hamburg (JSBACH) is a modular land surface scheme (Friedlingstein et al., 2006). It represents the land cover by distinguishing between 13 plant functional type (PFT)s (Raddatz et al., 2007) for present day's climate. Not all of these vegetation forms were present during the EOT, such as land use. For this thesis I modelled the PFTs shown in Table 1. During the EOT grass was not wide spread and did not appear on Antarctica (Strömberg, 2011). Therefore, in this work the PFTs C3 and C4 grass are also associated with mosses and lichens in a tundra environment.

Table 1: The here applied PFTs.

Level	PFT number	PFT description
1	2	tropical broadleaf evergreen
2	3	tropical broadleaf deciduous
3	4	extra-tropical evergreen
4	5	extra-tropical deciduous
5	10	raingreen shrubs
6	11	deciduous shrubs
7	12	C3 grass (associated with mosses and lichens)
8	13	C4 grass (associated with mosses and lichens)

The natural land cover change is modelled by the dynamic vegetation component within JSBACH (Reick et al., 2013).

OASIS3 coupler and ESM-tools

The coupling between the ocean and atmosphere model is done by the OASIS3 (Ocean Atmosphere Sea Ice Soil) coupler (Craig et al., 2017). This software offers very little intrusiveness in the application model codes and is therefore used in many different European ESMs (Valcke, 2013). The ESM-tool manage the technical framework, such as configuration and compiling (Barbi et al., 2021).

3.2. Topography and Bathymetry

The FESOM2 mesh and the input files for ECHAM6 and JSBACH are based on a reconstructed topography and bathymetry for the EOT shown in Figure 3. It is composed of three grids for different regions. The region of Antarctica is based on the minimum reconstruction by (Paxman et al., 2019), the Southern Ocean is based on (Hochmuth et al., 2020) and the global rest is taken from (Straume et al., 2020). The composition of these grids for this thesis was performed by Katharina Hochmuth. It has a resolution of 1° which corresponds to a resolution of ~ 5 km in the polar regions, a high resolution needed as the polar regions are of special interest.

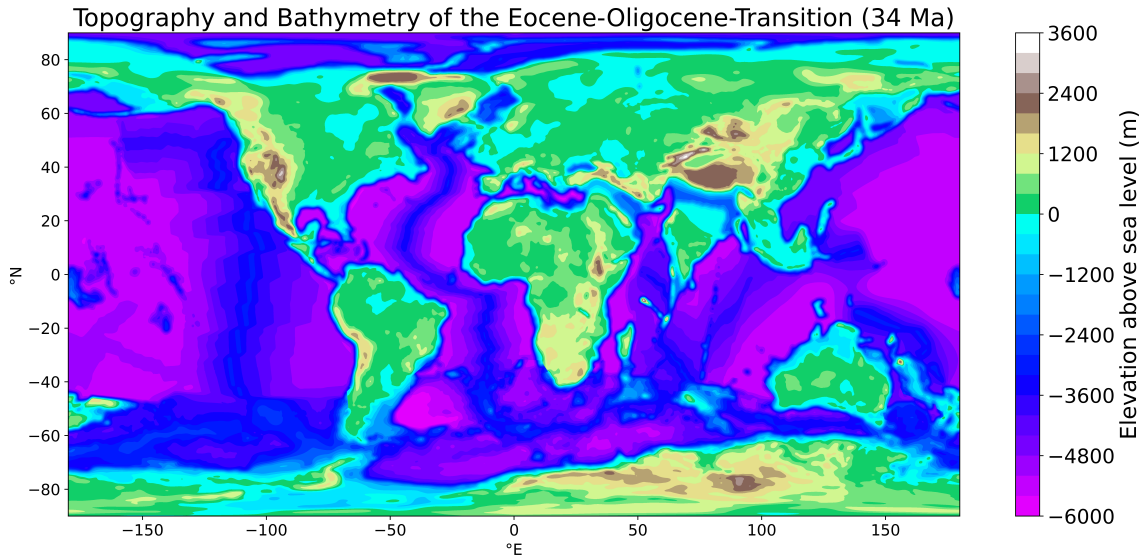


Figure 3: The reconstructed Bathymetry and Topography for the Eocene-Oligocene-Transition used for the model simulations

A closer look at the gateways present in this setup is important for the global ocean circulation and in particular for the circulation in the Southern ocean, as Southern passages began to open at that time (Sauermilch et al., 2021, Sijp et al., 2014). Other than today, in this EOT geography Tethys seaway and the Central American seaway are still open. The Tasmanian Gateway and the Drake passage are already open as shown in Figure 4. Both have a deepest depth of about 2000 m in a narrow section of about 2° . Thus, we expect the gateways to be too narrow to evoke the onset of a strong ACC which is described to happen ~ 4 Million years later (Scher et al., 2015). We chose the minimum

reconstruction by Paxman et al., 2019 because it fits well the findings from Klages et al., under review. These findings propose major parts of West Antarctica already lying below sea level and show potential for open trans-Antarctic sea ways. The Arctic ocean is not isolated from the other oceans in this set up. There is already a shallow Atlantic-Arctic oceanic gateway in the east of Greenland. The Greenland-Scotland Ridge is very narrow and shallow at that time, as well as Fram Strait. With a maximal depth of about 100 m in the shallowest part of the Fram Strait as shown in the cross section in Figure 4, only a low exchange of water can be expected here.

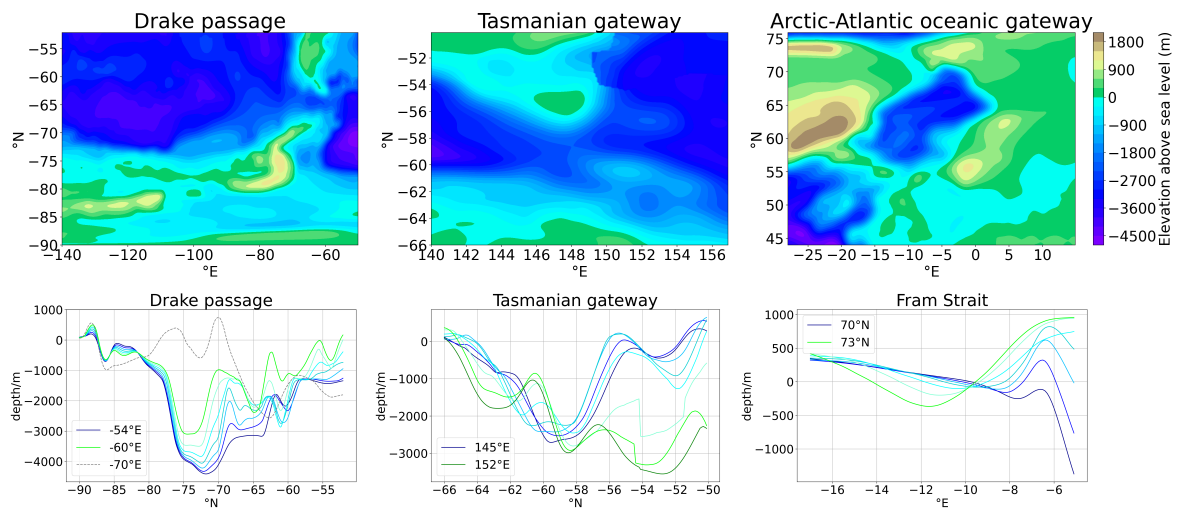


Figure 4: The topography and bathymetry in the region of three important gateways: (left) Drake passage, (centre) Tasmanian gateway, (right) Atlantic Arctic oceanic gateway. (Top) Map of the region, (bottom) cross section within the narrowest and flattest part

3.3. Model Runs

In this thesis I use the results from eight ESM runs, six for possible EOT conditions and two with a PI set up. These different model runs are listed in Table 2.

The general idea was to perform the model runs in three steps as shown in Figure 5. As there did not exist model runs with the AWI-ESM-2.1 set up, yet, the ESM started with very basic boundary conditions in step 1. The ocean started at rest, which means homogeneous temperature and salinity, using the specially created mesh (see Figure 2) and the EOT bathymetry (see Figure 3). The atmosphere and vegetation models started from general assumptions on insulation, vegetation and hydrological conditions based on

Table 2: Climate model runs by name, EOT of pre-industrial setup, CO₂ concentration relative to the PI conditions (1× = 274.8 ppm, 2× = 560 ppm, 3× = 840 ppm), ice sheet covering Antarctica and modelled years which were used (modelled but not used)

Name	Setup	PI CO ₂	Antarctic Ice	Model Years
PI1	PI	1×	PI	1000
EOT1	EOT	1×	no	250 (500)
EOT1ice	EOT	1×	PISM1	250
EOT2	EOT	2×	no	250 (500)
EOT2ice	EOT	2×	PISM2	250
EOT3	EOT	3×	no	250 (500)
EOT3ice	EOT	3×	PISM3	250
PI4	PI	4×	PI	630 (by Arpita Bose) (Bose, 2022)

the EOT topography (also see Figure 3). These assumptions do not include ice sheets, as indicated with 'no' in column 'Antarctic ice' in Table 2. These model runs are referred to as EOT(1,2,3) runs,

The results of these runs under different CO₂ conditions (1x, 2x and 3x with respect to the PI level) were utilized as the foundation for the AIS buildup. The ice sheet runs (step 2), here named PISM1, PISM2 and PISM3, were performed by Lu Niu.

In step 3 the equilibrated ice sheets from the PISM model runs were inserted as boundary conditions for the atmosphere model. For technical reasons the atmosphere and vegetation models could not be restarted from the previous climate runs. Therefore, I created new general atmospheric boundary conditions (now including the according Antarctic ice sheet, also indicated in Table 2). However, the ocean model could be restarted from the previous climate runs from the first lap. These ESM runs are referred to as EOTice runs.

The ESM ran for 250 model years (step 1), the ice model for 400,000 model years (step 2) and then again the ESM for 250 model years (step 3). As shown in Figure 6 (top) the ESM run has reached a quasi-equilibrium in the atmosphere and the ocean surface after 250 model years. The 2m air temperature and sea surface temperature is still rising slightly but no major changes are expected in further model years. The deep ocean has not quasi-equilibrated, yet. Figure 6 (bottom) shows that salinity in 1000 m depth is still decreasing significantly.

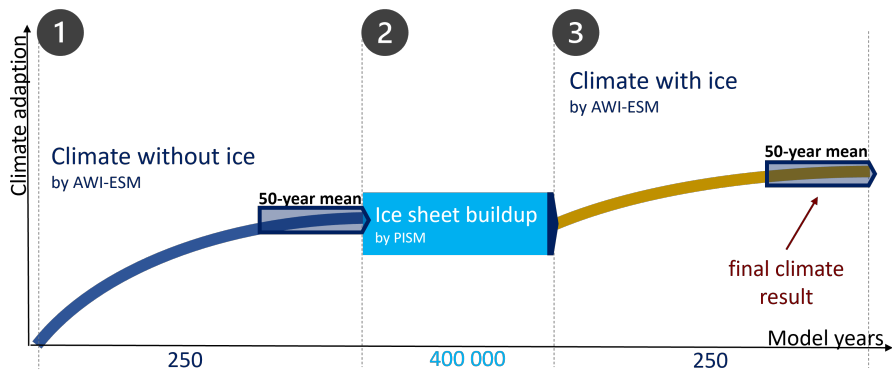


Figure 5: Order of the model runs including the PISM runs performed by Lu Niu

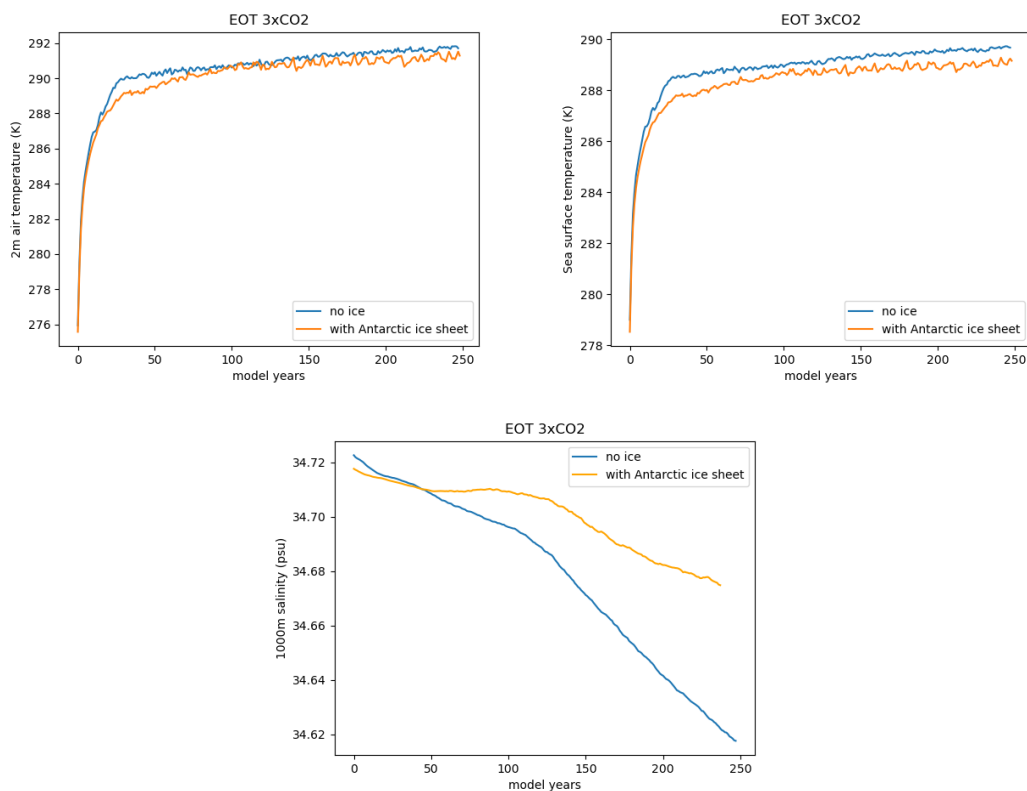


Figure 6: Quasi-equilibrium of the atmospheric model (top) exemplary shown for global annual mean 2m temperature (left) and sea surface temperature (right). The deep ocean has not yet reached the quasi-equilibrium, exemplary shown by the salinity in 1000 m of depth (bottom). All figures show 250 model years for the climate without and with Antarctic ice sheet with a CO_2 level of $3\times\text{PI}$.

4. Results

In this section I show the results of the eight different model runs. I present different climate parameters standing as representatives for the modelled climates during the EOT and the PI climates. The parameters air temperature, precipitation and vegetation are representatives for the atmospheric part. The oceanic part of the climate system is represented by ocean temperatures and currents, as well as, sea ice. First, I specifically focus on the Antarctic region. Second, I give an overview on the global climate.

4.1. Antarctic Climate in the EOT Model

The special interest in this thesis is the Antarctic climate and its interaction with the Antarctic ice sheet buildup.

4.1.1. Antarctic Ice

Figure 7 (left) shows the ice sheets used for the EOTice model simulations. The ice sheet growth was performed with PISM in the climate of the EOT no-ice runs under three different CO₂ conditions. The ice thickness is displayed in the colourscale from red to yellow. Underlying in blue and green colours is the bathymetry and topography which can be seen in Figure 17 in more detail.

For the highest CO₂ level of 3x PI conditions the ice sheet only covers parts of East-Antarctica, mainly today's Wilkes Land. On the lower CO₂ level of 2x PI the ice extends towards Enderby Land along the coast. A small ice cap then also covers Dronning Maud Land and Neuschwabenland. At the lowest CO₂ concentration of 1x PI these ice sheets grow towards the interior of the continent. The larger ice sheet even spreads up to the West coast of Antarctica, almost covering the whole continent. Also Antarctic Peninsula, which was an island at that time, was covered by glaciers up to 2000 m high. Only Coats Land remains ice free. The large EAIS even reaches about 4500 m of height in all three cases.

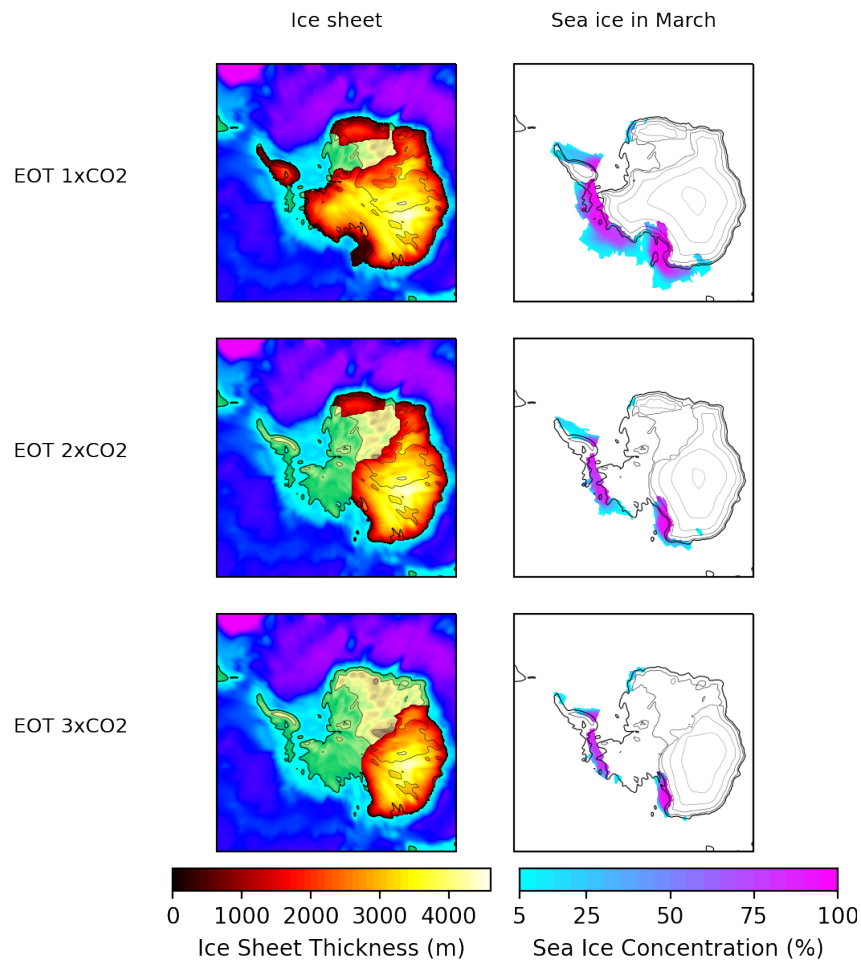


Figure 7: (left) Antarctic ice sheets from PISM runs with climate under the three different CO₂ levels. (right) Summer Antarctic sea ice of the EOTice runs.

There is only little sea ice present in summer for all CO₂ levels as can be seen in Figure 7 (right). The displayed data is the mean of the month march for the last 50 model years and there is only notable sea ice concentration along the West-Antarctic coast. For EOT1ice almost the whole West coast has some sea ice cover. Whereas, EOT3ice only holds sea ice in the Bellinghausen sea and along the East coast of Ross sea. There is a gap in the coastal region of the Weddel sea where no sea ice is displayed. This is due to interpolation problems of the plot programme and but could not be resolved in time. Sea ice is modelled in this region and according to SSTs in the Weddel sea (see Figure 9), sea ice can here be expected in the Western half of the basin.

4.1.2. Antarctic Temperatures

The direct comparison of the Antarctic summer climate without (left) and with Antarctic ice sheet (centre) is shown in Figure 8. On the right the difference of both runs for each CO₂ level is displayed. The effect of the ice sheet is very prominent. Especially, East Antarctic February 2m air temperature is up to 40°C lower in the EOTice runs. The biggest difference can be found in the 1xCO₂ runs. Contrasting, parts of the other Southern continents, such as Australia, South Africa and the Southern part of South America, are 5 – 15°C warmer than the no-ice runs. The air temperature above the ocean is slightly warmer (0 – 5°C) than in the no ice runs. Furthermore, the CO₂ effect, generally higher temperatures on higher CO₂ levels due to greenhouse warming, can be observed in the EOT runs, especially, in the EOTice runs.

In between the PI runs there are smaller differences. PI4 is slightly warmer over the ocean and Southern parts of Southern continents. While, over Antarctica itself PI4 is slightly colder than PI1. The EOT run which is best-comparable to the PI air temperatures is the EOT1ice run. All others are warmer.

The SSTs in the West Antarctic (Figure 9) during February lie around 0°C for the EOT1 runs and increase towards higher CO₂ levels. For EOT3ice they lie around 5°C, except for parts of the Weddel sea. An interesting feature which can be found in all EOT plots are warmer surface temperatures along the Eastern coasts of the Weddel and Ross sea. Warm water is transported into these basins by ocean currents as shown in Figure 10, the Weddel and the Ross gyre. The heat distribution changes within these gyres when the ice sheets enter the system. The West coasts of Weddel and Ross sea cool down as shown in Figure 9 (right). Also, the East Antarctic coast gets colder. Whereas, the Pacific sector gets warmer, in several spots up to 6°C. The warming effect is most present in the 1xCO₂ run, the cooling effect is strongest in the 3xCO₂ run. Again, the difference of the PI runs shows another pattern. PI4 SSTs are generally colder.

In the location of the Amundsen drill core (to which these model results are compared in section 5) I calculated the mean annual temperatures by taking the mean of the four next-neighbour grid cells. The results for 2m air temperature and water surface temperature belonging to the most important model runs are shown in Table 3. The

lowest temperatures can be found for PI1, the highest for EOT3ice. The EOTice runs differ by 7.1°C for air temperature and by 3.4°C for water temperature. The best-comparable runs in this location are EOT1ice and PI4, but due to technical reasons (see Appendix A PI4 results must be treated with caution).

Table 3: Annual mean temperatures at the location of the drill core (mean of four grid cells closest to drill location (see Figure 17)) for the EOTice and PI runs. The mean of the last 50 (*30) model years is taken

Run	2m Air Temperature (°C)	Water Surface Temperature (°C)
PI1	-10.3	-1.6
EOT1ice	-7,2	-0.8
EOT2ice	-2.6	1.0
EOT3ice	-0.1	2.6
PI4	-4.8*	-0.6*

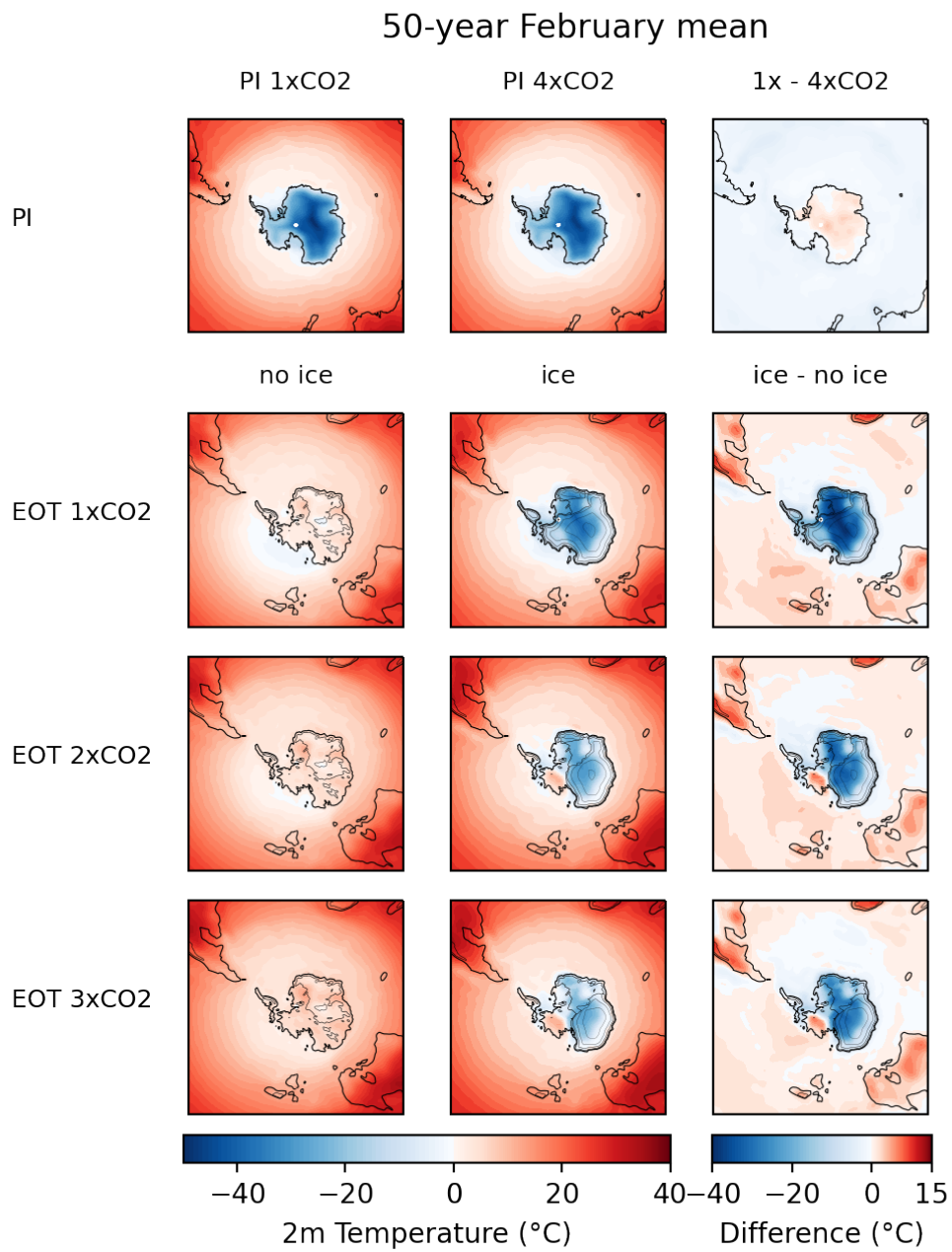


Figure 8: February mean 2m air temperatures over the Antarctic region

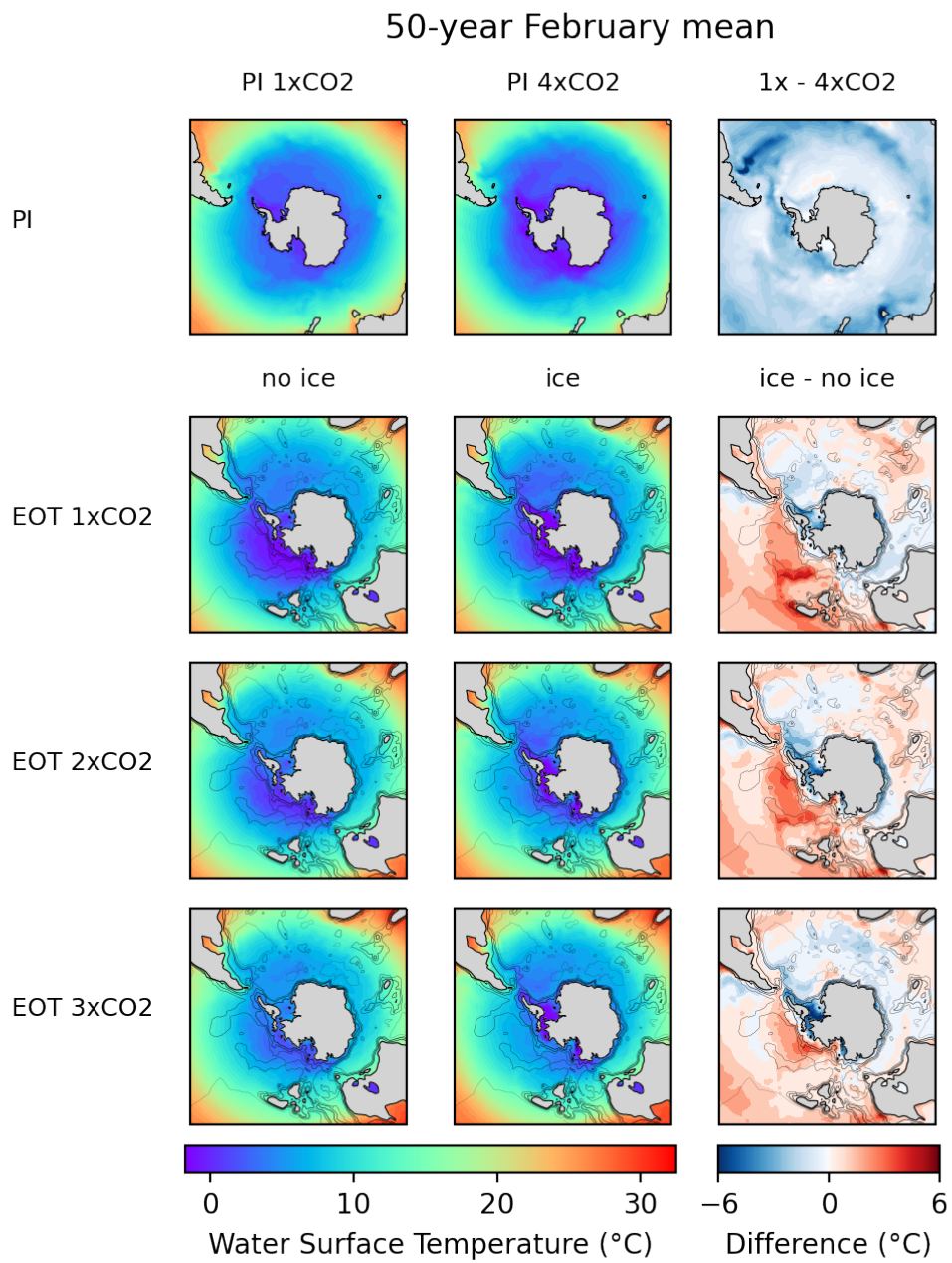


Figure 9: February mean water surface temperatures in the Southern ocean

4.1.3. Ocean Currents and Precipitation

Besides the observed Weddel and Ross gyre mentioned above, Figure 10 shows an Eastward circumpolar current in the Atlantic and Indian ocean. It starts in the Drake passage. After passing the passage the Eastward surface flow bends Northward, flows along the South American coast until it joins the circumpolar current. After passing the African continent and the Indic sector it proceeds through the Tasmanian gateway. In the Pacific ocean it gets weaker but still an Eastward trend can be observed.

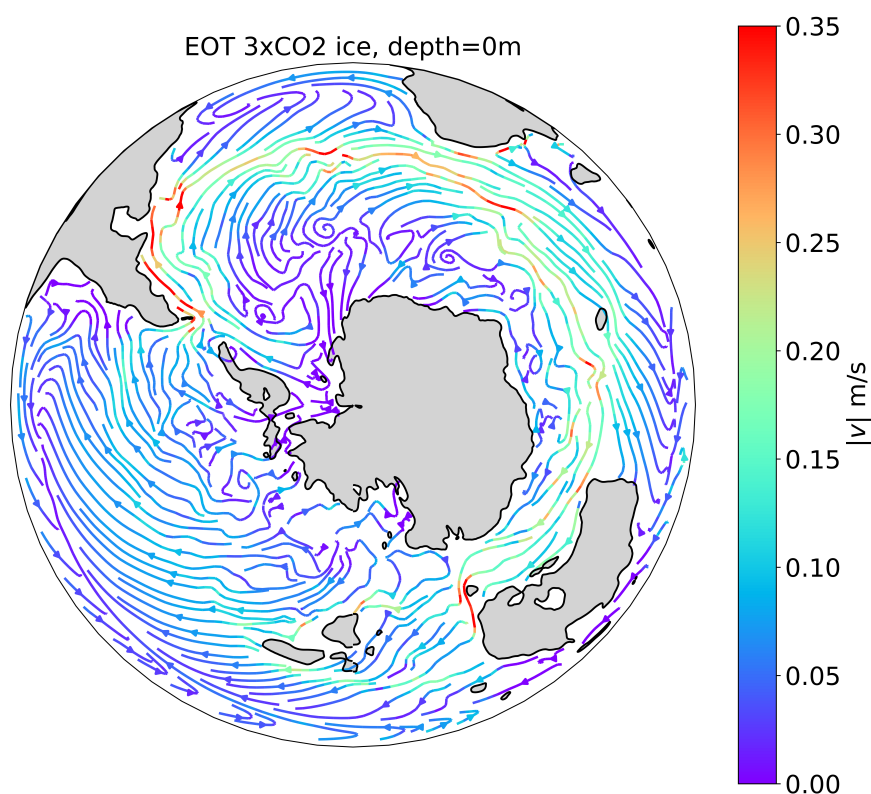


Figure 10: Streamplot of the ocean surface velocity

The precipitation in Figure 11 shows a rain belt circling Antarctica. High precipitation values appear above the circumpolar current (Figure 10). The highest amount of precipitation occurs on the West coast of the tip of South America. In presence of the ice sheet Figure 11 (right) precipitation decreases above the interior of the Antarctic continent. The central Antarctic then only experiences several dm of precipitation per year while the amount of precipitation increases over Wilkes Land towards the coast to more than 1

m/y. In the West Antarctic precipitation lies around 0.5 – 1 m/y, except for the Weddel Sea where it lies lower.

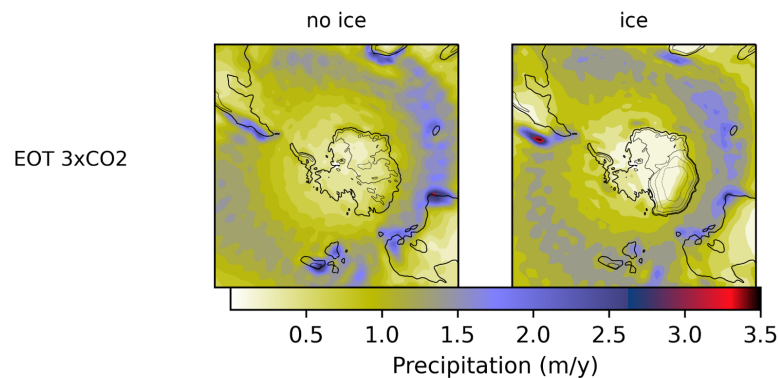


Figure 11: Annual total precipitation in the Antarctic region (large scale precipitation + convective precipitation)

4.2. Global Climate in the EOT Model

4.2.1. Global Temperatures

For direct comparison of all model runs I first take the global annual mean temperatures for the last 50 model years (in case of run PI4 I can only use the last 30 years). On the left side in Table 4 the global annual mean 2m air temperatures are shown, on the right side the according water surface temperatures. For better visualization these results are graphically prepared in Figure 12.

Table 4: Annual mean temperatures for the different model runs over the last 50 (*30) model years

Run	2m Air Temperature (°C)	Water Surface Temperature (°C)
PI1	13.1	13.5
EOT1	14.7	14.3
EOT1ice	13.5	13.5
EOT2	16.5	15.5
EOT2ice	16.2	14.9
EOT3	18.5	16.5
EOT3ice	18.0	15.9
PI4	15.8*	14.9*

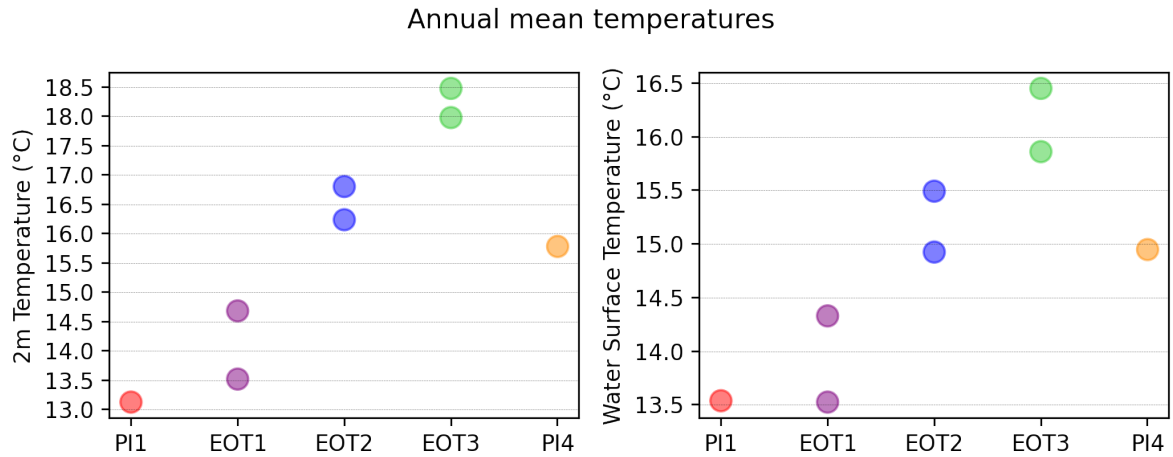


Figure 12: 2m air temperature and water surface temperature global annual means over the last 50 model years

All EOT model simulations shown here are warmer than the reference PI1 simulation in 2m air temperature and water surface temperature, or equal in case of the EOT1ice water temperature. The CO₂ effect due to greenhouse warming can be observed in Antarctic and global climate. The higher the CO₂ concentration, the higher the global mean temperatures within the same set ups. Furthermore, 2m air temperature is more sensitive to this effect than the water surface temperature, as air temperature rises are up to 2.7°C and water temperature changes are only up to 1.4°C. A second effect is the insert of the Antarctic ice sheets. It decreases the temperatures of the climate runs on equal CO₂ levels. This effect is largest for the EOT1 run, where air temperature decreases 1.2°C and water temperature decreases 0.8°C. For the runs with higher CO₂ levels both temperature changes range between 0.4 – 0.6°C. The PI4 air temperature is 2.7°C higher than the PI1 air temperature and the water temperature is 1.4°C higher in PI4 than in PI1. According to (Bose, 2022) the air temperature increase should be almost 7°C. The discrepancy might be explainable by technical reasons (see Appendix A). Therefore, the used PI4 data are not completely reliable and must be treated with caution.

Globally best-comparable runs from EOT and PI conditions differ compared to Antarctic best-comparable runs. According to the global annual mean temperatures the best-comparable runs are EOT1 (no AIS) and PI1. Whereas, the EOT2 run is best comparable to PI4 global mean temperatures.

The zonal mean temperatures in Figure 13 show a more differentiated picture on the tem-

perature differences of all runs. In the mid-latitudes the runs show only slight differences, whereas, in low and high latitudes major differences are present. The overall warmest run is EOT3, while there is no clear candidate for the overall coldest run.

The highest effect on zonal air temperature can be observed at the poles. All runs including an Antarctic ice sheet are coldest at the South pole with temperatures ranging between -50 to -30°C , whereas the EOT runs without an Antarctic ice sheet only reach temperatures down to -17°C . In contrast, for the North pole the pattern is not as clear as for the South pole. Still all EOT runs without Antarctic ice sheet are warmer than the according run on the same CO_2 level including an ice sheet, but the air temperature differences lie below 5°C . The lowest air temperatures here are not found in PI1 but the EOT1ice run. The highest air temperatures shows the EOT1 run, here, closely followed by the PI4 run. Overall, the CO_2 effect can be observed on all latitudes. Within a scenario higher CO_2 values always cause higher temperatures.

For the 50-year annual mean water surface temperature only slight changes can be seen in the Southern polar region, while major differences occur in the low latitudes. Here, CO_2 and ice effect can clearly be observed. The coldest run is EOT1ice, the warmest is EOT3. Around 30°N the PI temperatures decrease strongly towards higher latitudes, while the EOT runs show another peak in temperature. This peak is followed by a steep decrease. Around 60°N a more diverse pattern is shown with lowest temperatures in the EOT1ice run. The Arctic ocean temperatures then are all very similar again and lie around -2°C .

In Figure 14 the 50-year annual mean 2m air temperature is shown globally with the according land-sea mask. In general, the patterns look relatively similar in all runs. Over the oceans the air temperature gradually decreases towards higher latitudes, the only exception is a small stripe along the equator. The land masses have small-scale effects on the air temperature. Along the American West coast, along the Himalayas and within Southern Africa temperatures are lower than in the surrounding. Ice sheets have a great impact on the regional air temperature. The East Antarctic temperatures for the EOTice runs reach down to -50°C , while for the EOT runs without ice sheets only range around -10°C . In the PI runs the temperatures above the Antarctic ice sheet, as

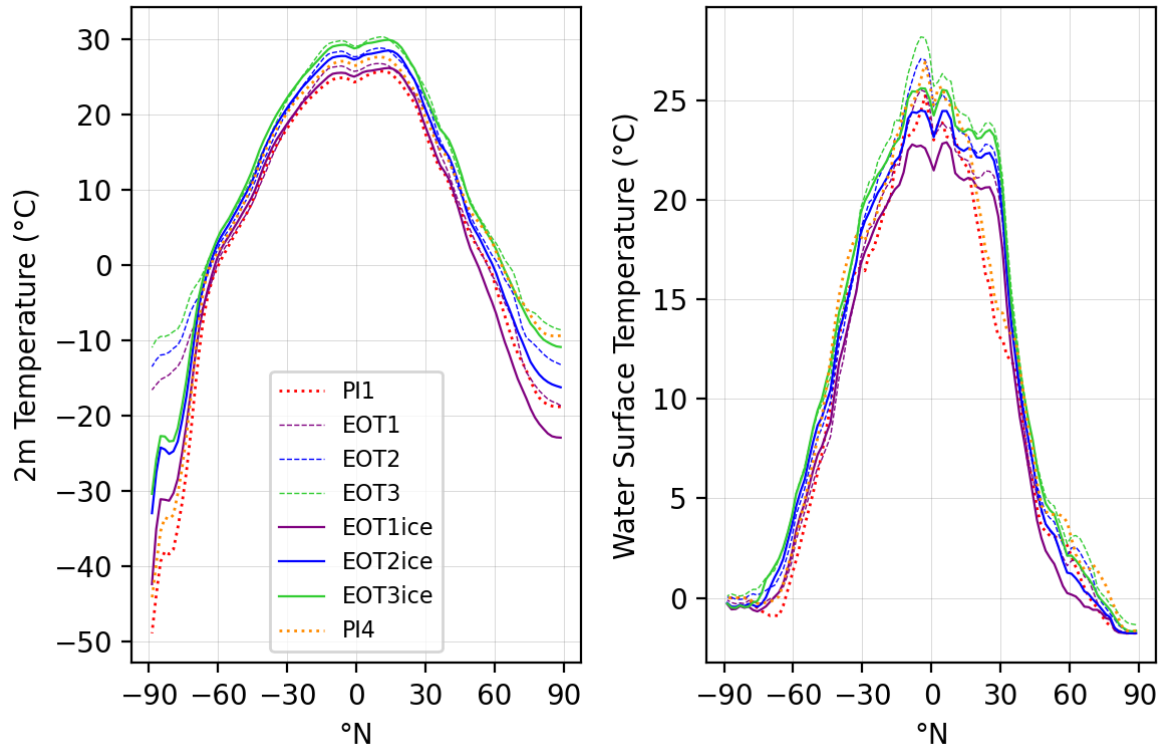


Figure 13: 50-year annual zonal mean 2m temperature and water surface temperatures for all model runs

well as, the Greenland ice sheet are low. In East Antarctica they are reaching down to -60°C .

Figure 15 displays the 50-year annual mean water surface temperature. An equatorial stripe of colder water is present in all runs in the Pacific, but in the EOT runs also in the Atlantic ocean. Otherwise, temperature decreases from $\pm 10^{\circ}\text{N}$ towards higher latitudes. In the PI runs warm surface water reaches high into the Arctic ocean towards the Arctic-Atlantic oceanic gateway, while, this effect can not be observed in the EOT runs. With increased atmospheric CO_2 concentration the Arctic oceans warms along the coast, which can also be seen in Figure 13 (right). Low latitude water surface temperatures also get higher under higher CO_2 concentrations. In EOT3 they reach up to 34°C . The Mediterranean sea is much warmer in EOT scenarios than in PI and within the EOT scenarios also the CO_2 effect is present.

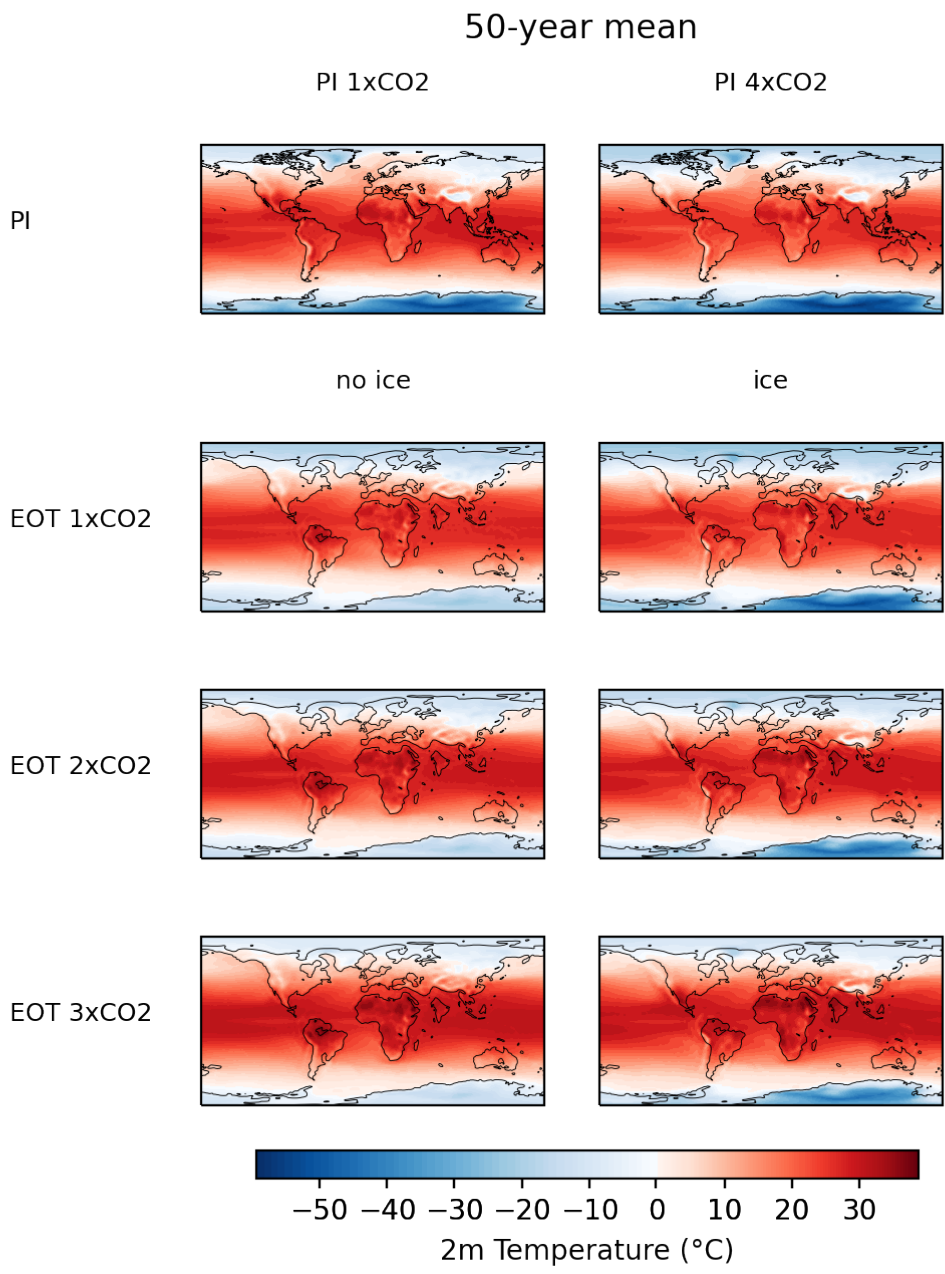


Figure 14: 50-year annual mean 2m air temperatures for all model runs

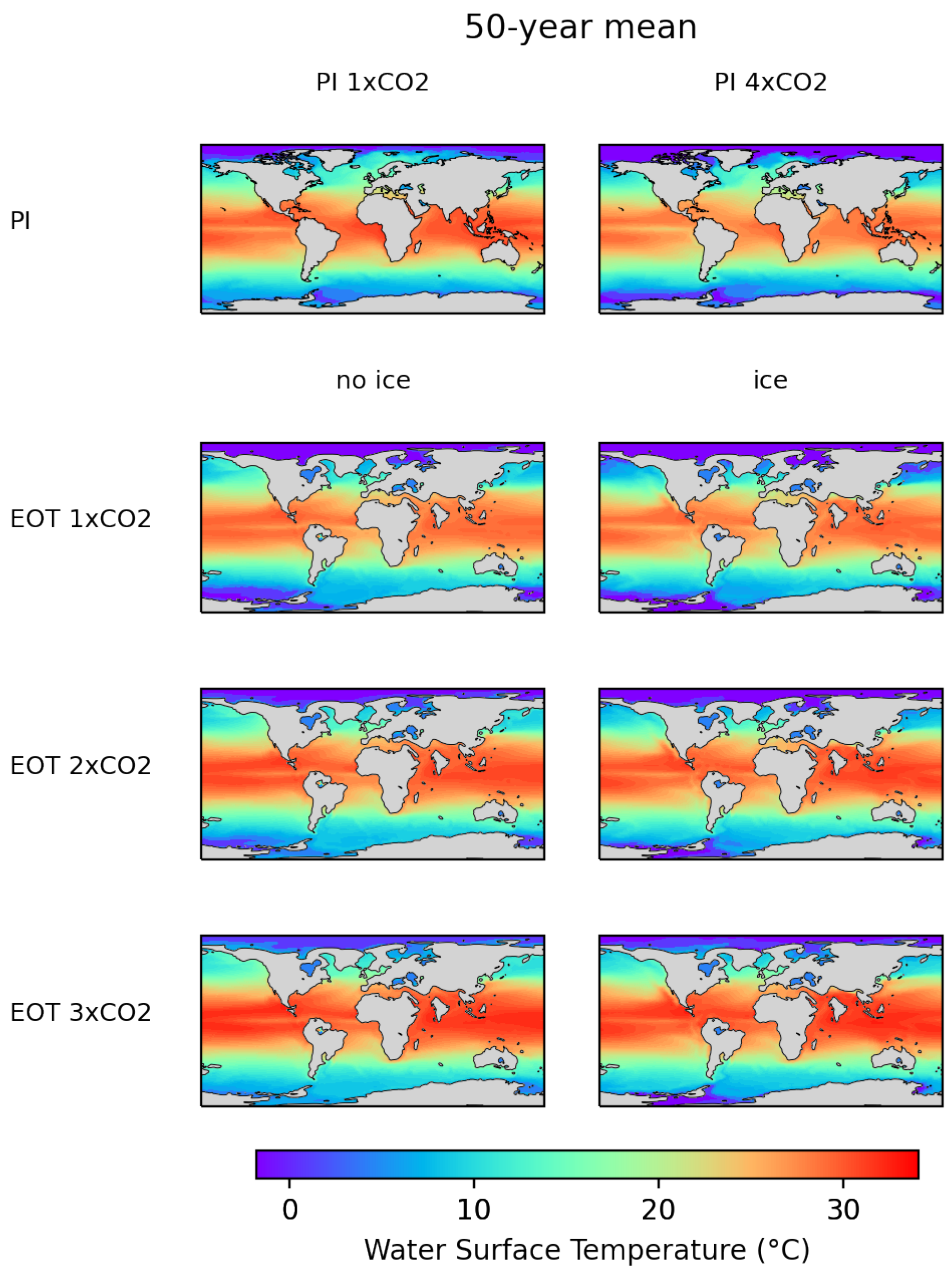


Figure 15: 50-year annual mean water surface temperatures for all model runs

4.2.2. Global Vegetation

The globally most dominant biomes are grass (or tundra) and shrubs. Mid-latitudes show lots of extra-tropical evergreen. Parts of Antarctica are covered by vegetation. C3 grass appears in low fractions and here is associated with mosses and lichens as grass has not reached Antarctica during the EOT, yet (Strömberg, 2011). Furthermore, Antarctica shows extra-tropical evergreen and deciduous shrubs. A more detailed description of global vegetation distribution and comparison to proxy data is shown in subsection 5.2.2.

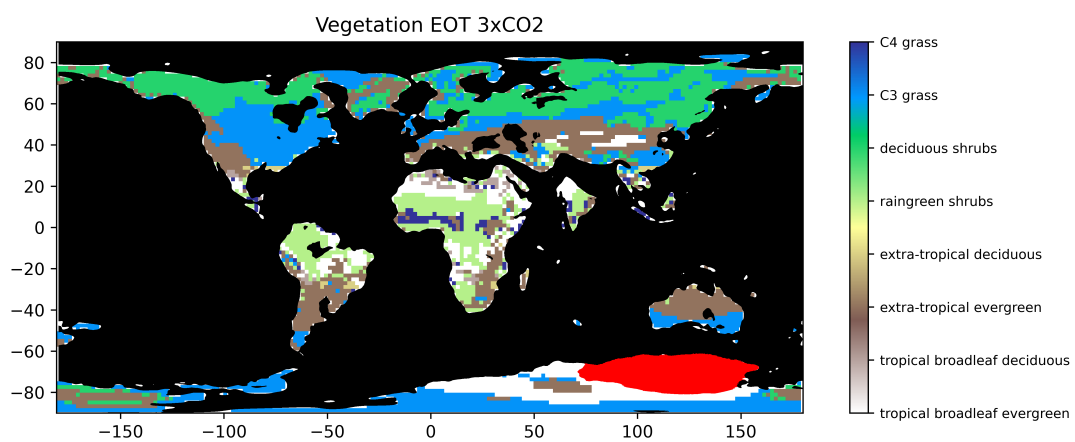


Figure 16: Maximal vegetation fraction per grid cell of the EOT3ice run. Red represents the extend of the ice sheet. White can also indicate no vegetation coverage like in the Antarctic.

5. Discussion

This work shows the climate results for EOT boundary conditions modelled by AWI-ESM-2.1. Under three different CO₂ levels (1x, 2x and 3x PI CO₂) an asymmetric ice sheet develops, only reaching continental scale for the lowest CO₂ level. West Antarctica is generally warmer than 0°C, East Antarctica colder. Only few summer sea ice is present and subpolar gyres and parts of an Eastward ACC develop. Global annual mean temperatures are higher than under PI conditions and eight different PFTs show the global vegetation distribution.

Meeting a good CO₂ level for the EOT simulations is fundamental for producing realistic ice and climate results (DeConto and Pollard, 2003). For this reason, primary the used CO₂ levels are discussed followed by the discussion of Antarctic climate and glaciation. The comparison of global climate and vegetation to other model and proxy data concludes the discussion.

5.1. Antarctic Climate and Ice Sheet

5.1.1. Reasonable Atmospheric CO₂ Concentrations

The reconstruction of Late Eocene atmospheric CO₂ concentrations delivers values ranging around 1000 ppm and is expected to be followed by a steep decrease during the EOT (Hutchinson et al., 2021). Proxy data for the EOT range between 400 – 1000 ppm (Hutchinson et al., 2021) and indicate a CO₂ level around 850 ppm (Pagani et al., 2011).

The glaciation of Antarctica is observed to show a CO₂ threshold behaviour. Proxy data propose a CO₂ threshold of ~ 600 ppm for a stable continental-scale AIS (Galeotti et al., 2016). However, the threshold of glaciation is also highly dependent on the model and the model configuration and can range between 560 – 920 ppm for intermediate glaciation (Gasson et al., 2014). A modelled threshold for ice sheet initiation is 600 – 840 ppm (DeConto and Pollard, 2003). Whereas, another model study proposes 900 ppm for a continental-scale ice sheet (Ladant et al., 2014). The opening of the gateways might also

have influenced the growth of the ice sheet. But the CO₂ concentration in the atmosphere is expected to play a more fundamental role in the extend of glaciation, as the opening effect depends on the CO₂ level at the timing of the opening (DeConto and Pollard, 2003). This supports the here used model set up of testing different CO₂ levels, while keeping a constant gateway configuration.

Summarising, the EOT runs with doubled and tripled CO₂ with respect to the PI level (560 and 840 ppm) are realistic scenarios. While, The EOT run on PI CO₂ level can more be seen as a test of the expected threshold behaviour and as a direct comparison to PI geographical conditions.

All scenarios show significant glaciation in the East Antarctic. Therefore, the threshold for the onset of glaciation in this model lies higher than 840 ppm. This meets the criteria of DeConto and Pollard, 2003. A continental-scale ice sheet reaching the coastline of West Antarctica is only seen for the lowest CO₂ scenario. Accordingly, the threshold for continental glaciation in this model is observed between 280 and 560 ppm. This is lower than the criteria of 600 ppm derived from proxy data but it joins the lower branch of modelled thresholds as it stays below modelled thresholds of > 560 ppm for intermediate glaciation (Gasson et al., 2014). The threshold of 900 ppm modelled by Ladant et al., 2014 can therefore be assumed as overestimated.

An explanation of the relatively low threshold for West Antarctic glaciation and the discrepancy to Ladant et al., 2014 could be different model set ups. In this study CO₂ is kept constant, while Ladant et al., 2014 uses a transient simulation. Also the topography plays an important role in ice sheet growth (see following discussion in subsection 5.1.3).

5.1.2. Comparison to Antarctic Climate in Drill Cores

The results from the sediment core discussed in (Klages et al., under review) lead to the idea to make the model runs presented in this work. In the following I compare the model results to those of the sediment core.

The sediment core was drilled in the Pine Island Through in the Amundsen Sea (site PS104-21). The location is shown in Figure 17 with respect to the used EOT bathymetry. The EOT sequence of the sediment core gives strong indications on West Antarctic ice conditions and temperatures of water and air. It shows no signs for a grounding ice sheet close to the drill site. Consequently, the WAIS cannot have been reaching anywhere close or did not even exist, yet (Klages et al., under review). The modelled climates on doubled and tripled CO₂ support this result. The model indicates no ice sheets in West Antarctica for 2x and 3xCO₂ levels. Also, no shelf ice is built up in Amundsen and Bellinghousen Sea. Therefore, the absence of rafting ice bergs in the Amundsen sediment core can also be supported. For 1xCO₂ the EAIS spreads into the West Antarctic even reaching the coast of Amundsen sea. Accordingly, the 1xCO₂ ice sheet seems overdeveloped. And, as discussed before 1xCO₂ is not a realistic boundary condition. A drill core from the Ross Sea indicates that there formed a marine-calving ice sheet ~ 32.8 Ma in the western Ross Embayment (Galeotti et al., 2016). Evidence for an EAIS is also found in Prydz bay (Zachos et al., 1992). This supports the location of all modelled EAISs.

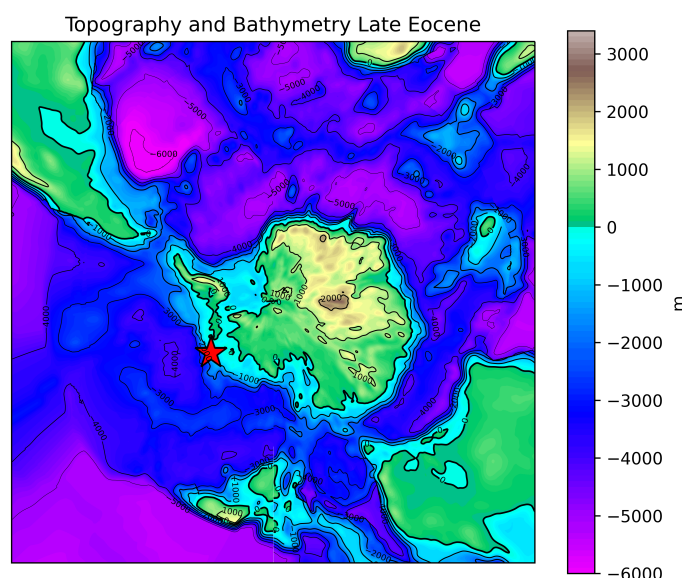


Figure 17: Approximate paleo-location of the sediment core (site PS104-21) in the Amundsen Sea (red star) with paleolatitude $\sim 73.5^\circ S$ (Klages et al., under review) in the used EOT topography and bathymetry

Furthermore, the Amundsen sea sediment core does not show signs of sea ice. The model shows only small regions of summer sea ice along the West Antarctic coast. Only the coldest regions (cf. Figure 8 and Figure 9) let sea ice develop. In the Ross sea, for instance, sea ice only develops along the Western coast. Cooling of air and SST by the nearby ice sheet and the Ross gyre and warming the Eastern Ross sea (cf. subsection 5.1.4) are reasonable explanations. Close to the drill site only the 1xPI CO₂ run shows sea ice, but in low concentration. Therefore, the model supports the sediment core results on ice sheets and sea ice very well.

The sediment core gives also clues about temperatures at the core site. The modelled temperatures turn out to be generally several degrees colder. The annual mean 2m air temperature in this location is reconstructed to be 6 – 8.5°C (Klages et al., under review). In contrast, the model supposes much lower air temperatures at the drill site for all CO₂ levels and times. The highest value delivers EOT3ice with –0.1°C. The mean SST is reconstructed to 6.2 – 10.5°C (Klages et al., under review) and modelled to max. 2.6°C (EOT3ice). The same trend applies to the summer air temperature. The modelled EOTice 2m air temperatures for February in the Amundsen Sea range between –5°C and +5°C Figure 8. These are lower than the proxy data from Klages et al., under review with a summer air temperature of 9.8 – 13.8°C. The comparison to other proxy data shows the same trend, air temperatures and SSTs are several degrees colder also in other regions of Antarctica (Klages et al., under review).

The discrepancy between model and proxy temperatures could be explained by several causes. On the one hand, proxy data come with uncertainties as the measurement itself and the evaluation method hold uncertainties, especially for polar regions in times this long ago. E.g., two methods are applied to the Amundsen sea drill core by (Klages et al., under review) with a difference of 1.5°C. On the other hand, the model data are based on uncertainties, too. The Southern gateway configuration is not completely resolved for that time period as it is the time of the opening of Drake passage and Tasmanian gateway. But, timing and deepening of the gateways plays a crucial role to ocean currents and heat transport (Sauermilch et al., 2021, Scher et al., 2015). Therefore, small changes in the gateway configuration can cause major changes in Antarctic temperatures. Furthermore, the orbital forcing has an important influence on ice sheet growth (Ladant et al., 2014). In

this work the orbital parameters are set equal to PI conditions while this might not have been suitable for the EOT. There are also uncertainties in the reconstructed topography (Paxman et al., 2019). As the next section will show, the topography has a substantial influence on the ice sheet, especially in West Antarctica. Also the calculation of the temperatures in the closest grid cells (Table 3) is prone to error, as the exact location is difficult to reconstruct and small regional and cyclic variations in the model can cause uncertainties.

Summing up this comparison, it can be stated that the best fit to the proxy data according to all criteria (ice sheet extend, sea ice and temperatures) is the EOT3ice run. The according ice sheet approximately meets the minimum estimate of global ice volume of 60% (Bohaty et al., 2012). The hypothesis of climate conditions allowing an asymmetric AIS with a major ice sheet in the East and minor or rather no ice in the West Antarctic is proven. Hence, more detailed climate research is undertaken on the model run EOT3ice in this work (ocean currents, precipitation, vegetation).

5.1.3. Comparison to other Glaciation Modelling Results

The comparison of the ice sheets with respect to the ice modelled by (Jamieson et al., 2010) for different Antarctic temperature scenarios shows similar signs for West-Antarctic glaciation restricted to higher mountains and also shows an ice nucleus in Dronning Maud Land. Jamieson et al., 2010 also observe an asymmetry in Antarctic glaciation with only little ice volume in the West but large amounts of ice in East Antarctica. But there are differences in the location of the largest ice nucleus. While (Jamieson et al., 2010) shows a nucleus around the Gamburtsev Mountains our model shows a nucleus in Wilkes Land, although, the Gamburtsev Mountains are present in our orography. Therefore, the ice sheet extends all the way to the coast of George V Land, while Jamieson et al., 2010 ice sheets do not reach the coast down to temperatures of -3.9°C .

The fact that parts of the Gamburtsev mountains are not covered by ice under 2x and 3xCO₂ conditions in this work is surprising. The mountains are more than 2000 m high Figure 17, the summer surface temperature is lower than in glaciated regions (in the climate runs with and without ice) Figure 8 and the annual amount of precipitation

is about 0.5 m/y Figure 11. This is less precipitation compared to the region of the nucleus in Northern Victoria Land or than along the coast of Wilkes Land but still not negotiable. A possible reason could be too few winter precipitation and would be worth further investigation.

The Antarctic topography has an important influence on the ice sheet build up (Van Breedam et al., 2022). (Wilson et al., 2013) use another topography with the Antarctic peninsula already connected to the main continent and the Transantarctic Mountains already present. Their ice sheet covers the whole continent and, therefore, does not show the asymmetry as strong as observed in this work. But still in Wilson et al., 2013 the thickness of the WAIS is half of the EAIS thickness and no bigger ice shelves are developed. The reason for using the minimum topography from Paxman et al., 2019 in this work is the consistency with the proxy data from Klages et al., under review.

Another model study using the same topography also shows an asymmetric AIS with a comparable extend of the EAIS (Vahlenkamp et al., 2018). But, the EAIS is shifted towards Dronning Maud land and does not cover Victoria Land. Different modelling methods and different states of equilibrium could be an explanation for that. They use transient simulations for CO₂. Their climate model runs without a dynamic ocean but the coupling to the ice sheet is regularly. Our model includes a dynamic ocean model which can describe the climate better in its complexity. But it needs several hundred model years to quasi-equilibrate and large computing capacity. For the deep ocean here quasi-equilibrium is not yet reached (section 3) and here constant CO₂ levels are applied to reduce complexity. Also the ice sheet is only coupled once to the climate and, therefore, is not equilibrated with the second climate run. Further coupling steps might still shift the ice sheet.

The best comparable ice sheet from (DeConto et al., 2007) is MEDICE. As discussed before, proxy data from the Amundsen sediment core supposes much higher summer 2m temperatures. Contrasting the summer air temperatures of both models are very similar. Above the ice sheet temperatures stay above -30°C and increase to $\sim 0^{\circ}\text{C}$ towards the coast. Above the ocean in West Antarctica the temperature stays around the freezing point or slightly above and then increases more or less circular towards lower

latitudes. Also, the summer sea ice shows similar patterns but our models develops a bit more sea ice cover in Bellinghausen sea for the EOT2ice run. This might be an effect of different coastlines. So, this work supports the conclusion by DeConto et al., 2007 that sea ice cooling feedbacks are not a necessary condition for Antarctic glaciation.

5.1.4. The Impact of Gateways

The Weddel and Ross gyre are found in all EOT simulations in different strengths (Figure 9 and Figure 10). They are expected to play a significant role in heat transport towards the pole at the time of the opening of Drake passage and Tasmanian gateway (Sauermilch et al., 2021). The model data shows warm surface water intruding into the Weddel sea along the Eastern coast. In the no-ice runs also the Western coast appears relatively warm and the centre shows lower temperatures which might be caused by Ekman upwelling (Sauermilch et al., 2021). While, the ice runs show a much colder Weddel sea with up to 6°C lower temperatures along the Western coast in the 3xCO₂ run. With an Antarctic ice sheet present the heat transport seems to be slowed down. The heat transport of the Weddel gyre might be one reason for the absence of an ice sheet in Coasts land in the 1xCO₂ run whilst most other parts of Antarctica are already covered in ice. The no-ice runs show relatively high air temperatures above Coasts land (see Figure 8).

Other than expected from the geography and previous work (Scher et al., 2015), the open Southern gateways already allow parts of an eastward ACC to develop (see Figure 10). In the Atlantic and Indic sector it is clearly observable. In the Pacific sector a slight Eastward trend is visible.

The circumpolar current seems to transport heat. SSTs are higher in regions the current is heading towards, like the Indic sector, the North coast of Australia and the Western side of Drake passage (see Figure 9). In these regions also high precipitation occurs (Figure 11). Clouds could be formed by evaporation from the warmer ocean, rising in warm air (Figure 8). This could explain the ice nucleus growth in Northern Victoria land.

Evidence for realistic precipitation in the West Antarctic can be found in the drill core from Klages et al., under review. The modelled precipitation close to the drill site is 1–1.5 m/y, exactly matching the proxy record of 1–2 m/y.

Evidently, this model simulations represent an intermediate state between the ACC regime blocking heat transport towards the pole (Barker and Thomas, 2004) and the subpolar gyre setting favouring heat transport into higher latitudes (Sauermilch et al., 2021).

5.2. Global Climate

5.2.1. Temperature Comparison to Proxy data and different models

Generally, the EOT climate is expected to be warmer than the PI climate (Pound and Salzmann, 2017). This work supports that in global annual mean Figure 12 and zonal mean temperatures Figure 13.

Compared to other models the global annual mean 2m air temperature tends to be lower in this model. For 2xCO₂ levels the temperature ranges between 16.5 – 25°C for other models (Hutchinson et al., 2021). This model provides 16.2°C for the EOT2ice run. The run without ice is slightly warmer with 16.5°C. For the 3xCO₂ scenario the comparison to mostly extrapolated data from other models (Hutchinson et al., 2021) show the same trend. One reason for that could be the relatively short model run time of 500 model years compared to 1000 – 9000 model years for the other models (Hutchinson et al., 2021). As Figure 6 shows, the model is in quasi-equilibrium for the atmosphere and ocean surface but temperatures are still rising slightly and the deep ocean is not equilibrated, yet. So, the temperatures might still rise in further model years and reach within the range of the compared models.

The comparison of modelled zonal mean SSTs (Figure 13) to proxy data show that all model runs are colder on high latitudes. The same anomaly is already observed for the Antarctic coast in subsection 5.1.2. Proxies show SSTs between 10 – 18°C for high latitudes (~ 60°N and S) (Hutchinson et al., 2021) where all model runs stay below 5°C.

Some possible reasons are already discussed in subsection 5.1.2. Also, there are high uncertainties how the Arctic climate responded to the EOT climate change (O'Regan et al., 2011). Proxy data North-West of Greenland show $13 - 15.4^{\circ}\text{C}$ for mean annual 2m temperature and $4.7 - 10^{\circ}\text{C}$ for SST for the Eocene (~ 45 Ma) (O'Regan et al., 2011). Modelled 2m temperatures for the EOT are more than 15°C lower but with respect to the 13 Ma discrepancy still conceivable. SSTs are only slightly colder with about 3°C . Due to very shallow Arctic-Atlantic gateways heat is not transported as far up into the North as under PI conditions (Figure 15). It is not evaluated if an Atlantic Meridional Overturning Circulation (AMOC) is possible under the given model conditions. This could be interesting for future work as the presence of an AMOC during the EOT is widely discussed (Vahlenkamp et al., 2018; Hutchinson et al., 2021).

On low latitudes ($30^{\circ}\text{S}-30^{\circ}\text{N}$) modelled and proxy SSTs show only slight differences. $20 - 33^{\circ}\text{C}$ are expected from proxies (Hutchinson et al., 2021) and modelled zonal SSTs range between $18 - 28^{\circ}\text{C}$. The general pattern of the modelled SSTs agrees well with the proxy data. Both show cold poles, steep increasing temperatures towards low latitudes, the highest temperatures South of the equator, a small decrease around the equator and constant high temperatures towards 30°N (Hutchinson et al., 2021). The best fit for low latitudes is the EOT3 run, followed by EOT2 and EOT3ice. So, the best run for the Antarctic region (EOT3ice) tends to be a bit too cold at high latitudes but still delivers acceptable results.

Figure 18 shows the impact of the AIS on the global 2m air temperature in this model. East Antarctica cools significantly by the direct cooling effect of the ice sheet, while the West Antarctic continent slightly warms. The air temperature above the Weddel sea decreases as already observed for the SST which might be caused by a weakening of the Weddel gyre (see subsection 5.1.4). The Pacific sector and Australia get warmer and large parts of the Arctic and the Northern-East Pacific cool. The same three effects are observed in the ensemble mean of different model runs discussed in Hutchinson et al., 2021. Differences to the ensemble mean are some of the warming patterns observed above the other continents, such as the American West coast, South Africa and Central Asia. Possible reasons for these anomalies could be changed wind and precipitation patterns along coasts through elevated orography in Antarctica. And in case of the Goby region

these wave pattern might show up due to different timings within cyclical variations. Despite these regional variations the ice sheet generally cools global climate. Global mean annual 2m air temperatures decrease by $0.5 - 1.3^{\circ}\text{C}$, SSTs decrease by $0.6 - 0.8^{\circ}\text{C}$ (Table 4).

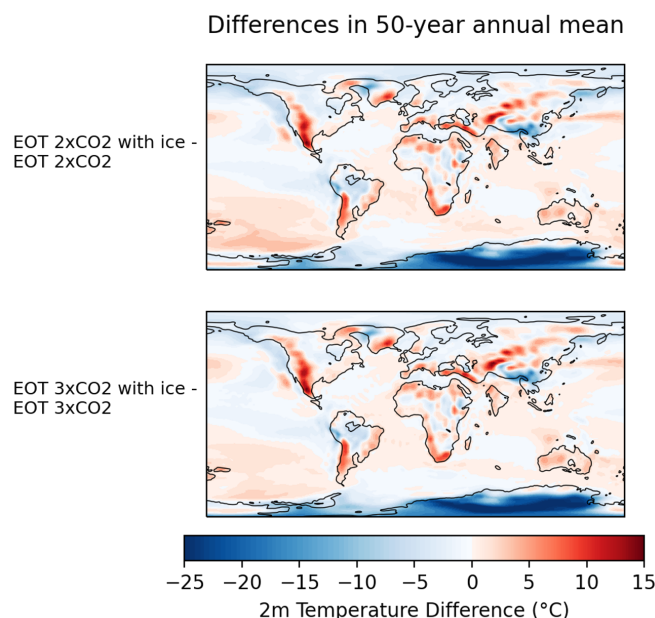


Figure 18: Difference in 2m air temperature between the ice and no-ice runs for 2x and 3x CO_2 levels

5.2.2. Global Vegetation Comparison to Proxy Data

Table 5 shows the comparison of the modelled PFTs to proxy data for the different continents. For most regions the model can only match the proxy data partly. Often the model shows less forest than expected. One reason for that might be that the modelled climate tends to be colder than the proxy data, especially towards higher latitudes. Therefore, vegetation zones might be shifted. Mixed forests can not be modelled. The according regions tend to develop more evergreen than deciduous. This might also be caused by the tendentially lower temperatures in the model. Please note that only the PFT with the highest coverage percentage per grid cell is displayed in Figure 16. Other PFTs could also appear in the same grid cell but are not shown here. Vegetation cover is also dependent on disturbances like forest fires which can change the PFTs on time scales of decades and distort the evaluation.

Good matches are found in Central Asia and Antarctica. The later provides the final confirmation for the hypothesis of a major ice sheet in East Antarctica and vegetation similar to the one in Patagonia nowadays in West Antarctica.

Table 5: Comparison of modelled PFTs and vegetation proxy data. Proxy data for Antarctica are taken from (Klages et al., under review) and the global rest from (Pound and Salzmann, 2017).

Region	Proxy data	modelled PFTs	Match?
North America			
North	Forest (cool- and warm-temperate mixed and subtropical evergreen)	deciduous shrubs, grass and some extra-tropical evergreen	partly
South	Tropical mangroves, swamps and forest	extra-tropical deciduous, grass and raingreen shrubs	ok
South America			
North	tropical evergreen forest	mainly raingreen shrubs and some tropical broadleaf evergreen	partly
South	cool-temperate shrubs and mixed forest	Extra-tropical evergreen and some C4 grass/tundra	partly
Africa			
North and South	? (significant gaps)	raingreen shrubs and tropical broadleaf deciduous	?
Central Africa	Tropical mangroves, swamps and forest, tropical evergreen forest	raingreen shrubs, grass and some extra-tropical evergreen	partly
Eurasia			
Eurasia	Mainly subtropical evergreen and warm-temperate mixed forest	North: deciduous shrubs and grass, lower latitudes: extra-tropical evergreen	partly
Central Asia	shrubs	grass and shrubs	good
South-East Asia	tropical mangroves, swamps and forest	various PFTs, best match is tropical broadleaf evergreen	partly
Australia			
Australia	Warm- and cool-temperate mixed forest	extra-tropical evergreen and grass	partly
Antarctica			
West Antarctica	deciduous forest, some shrubs, some tundra	deciduous shrubs, extra-tropical evergreen, tundra	good

6. Conclusion

The innovation of this work is tackling the uncertainty of EOT Antarctic glaciation by using the fully-coupled ESM AWI-ESM-2.1-LR with dynamic components for ocean, atmosphere and land surface coupled to the ice sheet model PISM. These simulations are motivated by new proxy data closing a data gap in West Antarctica (Klages et al., under review). The combination of model and proxy data strongly support the hypothesis of asymmetric Antarctic glaciation during the EOT. The comparison of ESM and proxy data verifies a good model performance for Antarctic climate and promising results for global climate - a proof that AWI-ESM-2.1-LR can perform reliable paleo climate simulations.

The expected CO₂ threshold behaviour of Antarctic glaciation is observed in this model. It is resolved by the comparison of three model runs on different CO₂ levels (280, 560 and 840 ppm). The threshold for the onset of glaciation here is in agreement with previous studies and lies above 840 ppm. The threshold for continental-scale glaciation reaching the West Antarctic coast in this model is relatively low compared to other models but still realistic with < 560 ppm.

Here follows a detailed summary of the climate results for Antarctica. The model run with tripled PI CO₂ and ice sheet (EOT3ice) agrees well with the proxy data. Ice sheet extend, sea ice, precipitation and vegetation of EOT3ice match the results from the Amundsen sea sediment core (Klages et al., under review). On high latitudes (North and South) the modelled air and sea surface temperatures are several degrees lower than proxy data propose (Klages et al., under review, Hutchinson et al., 2021). But this discrepancy does not disprove the model because various uncertainties have to be considered. Proxy data carry uncertainties and boundary conditions of the model, like gateway configuration, topography and orbital forcing are based on assumptions and reconstructions.

As expected, the modelled Antarctic and global climate are generally warmer than PI climate (almost +5°C). This climate allows a major EAIS to grow. This EAIS is not a continental-scale ice sheet and does not reach into West Antarctica. East Antarctic

summer 2m air temperatures are below, West Antarctic mostly above 0°C. West Antarctic summer SSTs range around 0 – 5°C along the coast only allowing few summer sea ice. The Southern gateways are open but narrow. Unexpectedly, this configuration already supports an intermediate state between subpolar gyres and ACC for the Southern ocean. Subpolar gyres warm the East coasts of Weddel and Ross sea as observed in previous work (Sauermilch et al., 2021). Concurrently, the ACC has already partly developed other than proposed by Scher et al., 2015. This Eastward current seems to transport heat. In regions the current is heading to surface ocean and air temperatures are increased and more precipitation is produced.

The modelled global climate tends to be colder than comparable modelled EOT climate. Nevertheless, global vegetation can be partly resolved and further model years and deep ocean quasi-equilibrium might contribute to even better results.

Concluding, the combination of proxy data from Klages et al., under review and this work provides an important contribution to current research on the climate of the EOT and the build up of the AIS. The observation of the AIS asymmetry during the warmer climate of the EOT found in this work could also be an interesting reference for future scenarios of Antarctic ice sheets.

7. Recommendations

The ESM produces a huge variety of output data. In this work I analysed some basic climate variables and especially focussed on the Antarctic region. On the available data more analysis could be performed to get a wider picture on the modelled global climate.

The Southern Ocean is here found to be in an intermediate state between an subpolar gyre and ACC regime. As further evaluation for quantitative comparison to other studies would serve the calculation the barotropic stream function in the Southern ocean. This could also prove the hypothesis of the ice sheet weakening the subpolar gyres.

It is widely discussed whether during the EOT already an AMOC was established or not (Hutchinson et al., 2021). The closing of the Barents seaway and the deepening of the Greenland-Scotland Ridge are traded as possible trigger for the onset of the AMOC (Vahlenkamp et al., 2018). In this set up the Greenland-Scotland Ridge is open but very shallow with about 100 m at the shallowest point (see Figure 4 (right)) compared to a modelled threshold of 200 m (Vahlenkamp et al., 2018). The Barents seaway is shallow but open in this set up Figure 4 (right). The question is if substantial water exchange is happening here. Also other boundary conditions effect the AMOC such as CO₂ forcing or Southern Ocean gateway changes (Hutchinson et al., 2021). Therefore, an investigation of the stream function and heat transport in the Atlantic ocean for this model would be an interesting next step.

A further point of investigation could be seasonal Arctic sea ice analysis. The modelled Arctic ocean should be cold enough for at least developing winter sea ice (see Figure 15). The seasonal behaviour during the EOT could give reference for Arctic sea ice in warm climates and could contribute to prediction of future Arctic sea ice development.

The model runs itself could also be extended in different ways to improve and widen the expressive power of the model results. Longer model runs of 1000 years are favourable to also reach deep ocean quasi-equilibrium. This is particularly important for observing the deep water formation. Also more coupling steps with the ice sheet model are necessary

to equilibrate climate and ice sheet, as the growth of the Antarctic ice sheet might have had a bigger impact on Southern deep water formation than the gateway configuration (Goldner et al., 2014).

For comparison, a similar model run with a CO₂ level of 4x PI conditions (~ 1120 ppm) could also be interesting as the exact CO₂ level during the EOT remains uncertain and the Late Eocene is expected to show a CO₂ concentration around 1000 ppm (Anagnostou et al., 2016). This could show whether the onset of glaciation even occurs on such a high atmospheric CO₂ concentration or only on lower levels as simulated in this work.

As the atmospheric CO₂ level performed a potentially steep decrease during the EOT (Hutchinson et al., 2021) and did not remain on a stable level as in the model runs performed in this work, a transient simulation with gradually decreasing CO₂ concentrations or reconstructed transient CO₂ levels like in Van Breedam et al., 2022 could be of interest. Such transient simulations could show if changing CO₂ and temperatures change the way the ice sheet develops.

As ice volume increased substantially during the EOT (Bohaty et al., 2012) and the West Antarctic is here found to only have a minor contribution, the question arises whether other regions in the Northern hemisphere might have glaciated during the EOT, as well. Other model data argue against bipolar glaciation, while some proxy data show signs for small glaciers on Greenland (Hutchinson et al., 2021). Therefore, Arctic ice sheet modelling might also be interesting future research. It then must be considered that the CO₂ threshold for Arctic glaciation is expected to be significantly lower than the Antarctic threshold (DeConto et al., 2008).

The model is also relying on boundary conditions which can have significant impact on the model results. There are still high uncertainties on the EOT bathymetry, especially on the opening and deepening of the Drake passage (Livermore et al., 2007). The Southern gateways play an important role in Southern ocean circulation and heat transport (Sauermilch et al., 2021). Further reconstruction research would help to improve the model results on heat transport and, therefore, provide more reliable results on the development of the Antarctic ice cover.

Also, the topography has a significant influence on the ice sheet build up, especially on the WAIS as the comparison to (Wilson et al., 2013) shows. And, there are still uncertainties in the reconstruction (Paxman et al., 2019). Therefore, further reconstruction research on the West Antarctic topography will enhance the reliability of the modelled onset of West Antarctic glaciation.

Acknowledgments

Many thanks to...

- ... my family and friends, especially my parents for making my studies possible, supporting and motivating me and for taking an active interest in what I am actually doing.
- ... my supervisors Gerrit Lohmann, Johann Klages and my technical supervisor Paul Gierz for giving me the chance on this fascinating and challenging topic and their support during my thesis.
- ... Lu Niu for the uncomplicated and supportive co-work with the ice sheet modelling.
- ... Katharina, Uta, Christian, Akil, Arpita, Kowiy, Lilly, Martin, Sven, Ronja, Umesh, Rebecca, Janina, Fernanda and all the others who helped me out with data, input files, the model set up, python scripts, nice talks...

References

- Anagnostou, E. et al. (2016). “Changing atmospheric CO₂ concentration was the primary driver of early Cenozoic climate”. In: *Nature* 533, pp. 380–384. DOI: 10.1038/nature17423.
- Barbi, D. et al. (2021). “ESM-Tools version 5.0: a modular infrastructure for stand-alone and coupled Earth system modelling (ESM)”. In: *Geoscientific Model Development* 14.6, pp. 4051–4067. DOI: 10.5194/gmd-14-4051-2021.
- Barker, P. and Thomas, E. (2004). “Origin, signature and palaeoclimatic influence of the Antarctic Circumpolar Current”. In: *Earth-Science Reviews* 66.1, pp. 143–162. ISSN: 0012-8252. DOI: 10.1016/j.earscirev.2003.10.003.
- Bohaty, S. M. et al. (2012). “Foraminiferal Mg/Ca evidence for Southern Ocean cooling across the Eocene–Oligocene transition”. In: *Earth and Planetary Science Letters* 317-318, pp. 251–261. ISSN: 0012-821X. DOI: 10.1016/j.epsl.2011.11.037.
- Bose, A. (2022). “Quantification of the impact of adjusted ozone climatology on a warmer than present climate simulated by AWI-ESM-2.1-LR”. Alfred-Wegener Institute, University of Bremen.
- Craig, A. et al. (2017). “Development and performance of a new version of the OASIS coupler, OASIS3-MCT_3.0”. In: *Geoscientific Model Development* 10.9, pp. 3297–3308. DOI: 10.5194/gmd-10-3297-2017.
- Danilov, S. et al. (2017). “The Finite-volumE Sea ice–Ocean Model (FESOM2)”. In: *Geoscientific Model Development* 10.2, pp. 765–789. DOI: 10.5194/gmd-10-765-2017.
- DeConto, R. and Pollard, D. (2003). “Rapid Cenozoic glaciation of Antarctica induced by declining atmospheric CO₂”. In: *Nature* 421.6920, pp. 245–249. DOI: 10.1038/nature01290.
- DeConto, R. et al. (2007). “Sea ice feedback and Cenozoic evolution of Antarctic climate and ice sheets”. In: *Paleoceanography* 22.3. DOI: 10.1029/2006PA001350.

- DeConto, R. et al. (2008). “Thresholds for Cenozoic bipolar glaciation”. In: *Nature* 455.3. DOI: 10.1038/nature07337.
- Friedlingstein, P. et al. (2006). “Climate-carbon cycle feedback analysis: Results from the C4MIP model intercomparison”. In: *Journal of Climate* 19, pp. 3337–3353. DOI: 10.1175/JCLI3800.1.
- Galeotti, S. et al. (2016). “Antarctic Ice Sheet variability across the Eocene-Oligocene boundary climate transition”. In: *Science* 352.6281, pp. 76–80. DOI: 10.1126/science.aab0669.
- Gasson, E. et al. (2014). “Uncertainties in the modelled CO₂ threshold for Antarctic glaciation”. In: *Climate of the Past* 10.2, pp. 451–466. DOI: 10.5194/cp-10-451-2014.
- Goldner, A. et al. (2014). “Antarctic glaciation caused ocean circulation changes at the Eocene–Oligocene transition”. In: *Nature* 511.7511, pp. 574–577.
- Hochmuth, K. et al. (2020). “The evolving paleobathymetry of the circum-Antarctic Southern Ocean since 34 Ma: A key to understanding past cryosphere-ocean developments”. In: *Geochemistry, Geophysics, Geosystems* 21.e2020GC009122. DOI: 10.1029/2020GC009122.
- Hutchinson, D. K. et al. (2021). “The Eocene–Oligocene transition: a review of marine and terrestrial proxy data, models and model–data comparisons”. In: *Climate of the Past* 17.1, pp. 269–315. DOI: 10.5194/cp-17-269-2021.
- Jamieson, S. S. et al. (2010). “The evolution of the subglacial landscape of Antarctica”. In: *Earth and Planetary Science Letters* 293.1, pp. 1–27. ISSN: 0012-821X. DOI: 10.1016/j.epsl.2010.02.012.
- Klages, J. et al. (under review). “Asymmetry in Antarctic ice sheet cover during the early Oligocene glacial maximum”. In: *under review for Nature Geoscience*.
- Koldunov, N. V. et al. (2019). “Scalability and some optimization of the Finite-volume Sea ice–Ocean Model, Version 2.0 (FESOM2)”. In: *Geoscientific Model Development* 12.9, pp. 3991–4012. DOI: 10.5194/gmd-12-3991-2019.

- Ladant, J.-B. et al. (2014). “The respective role of atmospheric carbon dioxide and orbital parameters on ice sheet evolution at the Eocene-Oligocene transition”. In: *Palaeoceanography* 29.8, pp. 810–823. DOI: 10.1002/2013PA002593.
- Livermore, R. et al. (2007). “Drake Passage and Cenozoic climate: An open and shut case?” In: *Geochemistry, Geophysics, Geosystems* 8.1. DOI: 10.1029/2005GC001224.
- O’Regan, M. et al. (2011). “A Synthesis of the Long-Term Paleoclimatic Evolution of the Arctic”. In: *Oceanography* 24, pp. 66–80. DOI: 10.5670/oceanog.2011.57.
- Pagani, M. et al. (2011). “The Role of Carbon Dioxide During the Onset of Antarctic Glaciation”. In: *Science* 334, pp. 1261–1264.
- Paxman, G. J. G. et al. (2019). “Reconstructions of Antarctic topography since the Eocene-Oligocene boundary”. In: *Palaeogeography Palaeoclimatology Palaeoecology* 535.109346. DOI: 10.1016/j.palaeo.2019.109346.
- Pound, M. J. and Salzmann, U. (2017). “Heterogeneity in global vegetation and terrestrial climate change during the late Eocene to early Oligocene transition”. In: *Scientific Reports* 7.1. DOI: 10.1038/srep43386.
- Raddatz, T. et al. (2007). “Will the tropical land biosphere dominate the climate–carbon cycle feedback during the twenty-first century?” In: *Climate Dynamics* 29 (6), pp. 565–574. DOI: 10.1007/s00382-007-0247-8.
- Reick, C. et al. (2013). “The representation of natural and anthropogenic land cover change in MPI-ESM”. In: *Journal of Advances in Modeling Earth Systems* 5.3, pp. 459–482. DOI: 10.1002/jame.20022.
- Sauermilch, I. et al. (2021). “Gateway-driven weakening of ocean gyres leads to Southern Ocean cooling”. In: *Nature Communications* 12.6465. DOI: 10.1038/s41467-021-26658-1.
- Scher, H. D. et al. (2015). “Onset of Antarctic Circumpolar Current 30 million years ago as Tasmanian Gateway aligned with westerlies”. In: *Nature* 523, pp. 580–583. DOI: 10.1038/nature14598.
- Scholz, P. et al. (2019). “Assessment of the Finite-volume Sea ice-Ocean Model (FESOM2.0) – Part 1: Description of selected key model elements and comparison to

- its predecessor version”. In: *Geoscientific Model Development* 12.11, pp. 4875–4899. DOI: 10.5194/gmd-12-4875-2019.
- Sidorenko, D. et al. (2015). “Towards multi-resolution global climate modeling with ECHAM6–FESOM. Part I: model formulation and mean climate”. In: *Climate Dynamics* 44.3, pp. 757–780. DOI: 10.1007/s00382-014-2290-6.
- Sijp, W. P. et al. (2014). “The role of ocean gateways on cooling climate on long time scales”. In: *Global and Planetary Change* 119, pp. 1–22. ISSN: 0921-8181. DOI: 10.1016/j.gloplacha.2014.04.004.
- Stevens, B. et al. (2013). “Atmospheric component of the MPI-M Earth System Model: ECHAM6”. In: *JAMES* 5.2, pp. 146–172. DOI: 10.1002/jame.20015.
- Straume, E. O. et al. (2020). “Global Cenozoic Paleobathymetry with a focus on the Northern Hemisphere Oceanic Gateways”. In: *Gandwana Research* 86, pp. 126–143. DOI: 10.1016/j.gr.2020.05.011.
- Strömberg, C. A. (2011). “Evolution of Grasses and Grassland Ecosystems”. In: *Annual Review of Earth and Planetary Sciences* 39.1, pp. 517–544. DOI: 10.1146/annurev-earth-040809-152402.
- Vahlenkamp, M. et al. (2018). “Ocean and climate response to North Atlantic seaway changes at the onset of long-term Eocene cooling”. In: *Earth and Planetary Science Letters* 498, pp. 185–195. ISSN: 0012-821X. DOI: 10.1016/j.epsl.2018.06.031.
- Valcke, S. (2013). “The OASIS3 coupler: a European climate modelling community software”. In: *Geoscientific Model Development* 6.2, pp. 373–388. DOI: 10.5194/gmd-6-373-2013.
- Van Breedam, J. et al. (2022). “Modelling evidence for late Eocene Antarctic glaciations”. In: *Earth and Planetary Science Letters* 586, p. 117532. ISSN: 0012-821X. DOI: <https://doi.org/10.1016/j.epsl.2022.117532>.
- Wallace, J. and Hobbs, P. (2006). *Atmospheric Science: An Introductory Survey*. International geophysics series. Elsevier Academic Press. ISBN: 9780127329512.

Wilson, D. S. et al. (2013). “Initiation of the West Antarctic Ice Sheet and estimates of total Antarctic ice volume in the earliest Oligocene”. In: *Geophysical Research Letters* 40.16, pp. 4305–4309. DOI: 10.1002/grl.50797.

Zachos, J. C. et al. (1992). “Early Oligocene ice-sheet expansion on Antarctica: Stable isotope and sedimentological evidence from Kerguelen Plateau, southern Indian Ocean”. In: *Geology* 20.6, pp. 569–573. ISSN: 0091-7613. DOI: 10.1130/0091-7613(1992)020<0569:EOISE0>2.3.CO;2.

A. Technical Details

All deep time runs were started with a PI orography and the target orography Late Eocene for the first two years. For the climate without ice runs all moist layers in the jsbach input file were set to 0.

The PI 4xCO₂ run was performed under the setting `default-output=True` which causes that some variables write a snapshot of a single day instead of a monthly mean to the output. Therefore, it is not directly comparable to the other output data and must be treated with care.

Declaration

Offizielle Erklärungen von

Name: Hanna Sophie Knahl

Matrikelnr.: 3224379

Eigenständigkeitserklärung

Ich versichere, dass ich die vorliegende Arbeit selbstständig verfasst und keine anderen als die angegebenen Quellen und Hilfsmittel verwendet habe. Alle Teile meiner Arbeit, die wortwörtlich oder dem Sinn nach anderen Werken entnommen sind, wurden unter Angabe der Quelle kenntlich gemacht. Gleiches gilt auch für Zeichnungen, Skizzen, bildliche Darstellungen sowie für Quellen aus dem Internet. Die Arbeit wurde in gleicher oder ähnlicher Form noch nicht als Prüfungsleistung eingereicht. Die elektronische Fassung der Arbeit stimmt mit der gedruckten Version überein. Mir ist bewusst, dass wahrheitswidrige Angaben als Täuschung behandelt werden.

A) Erklärung zur Veröffentlichung von Bachelor- oder Masterarbeiten

Die Abschlussarbeit wird zwei Jahre nach Studienabschluss dem Archiv der Universität Bremen zur dauerhaften Archivierung angeboten. Archiviert werden:

1) Masterarbeiten mit lokalem oder regionalem Bezug sowie pro Studienfach und Studienjahr 10 % aller Abschlussarbeiten

2) Bachelorarbeiten des jeweils ersten und letzten Bachelorabschlusses pro Studienfach u. Jahr.

x Ich bin damit einverstanden, dass meine Abschlussarbeit im Universitätsarchiv für wissenschaftliche Zwecke von Dritten eingesehen werden darf.

x Ich bin damit einverstanden, dass meine Abschlussarbeit nach 30 Jahren (gem. §7 Abs. 2 BremArchivG) im Universitätsarchiv für wissenschaftliche Zwecke von Dritten eingesehen werden darf.

Ich bin nicht damit einverstanden, dass meine Abschlussarbeit im Universitätsarchiv für wissenschaftliche Zwecke von Dritten eingesehen werden darf.

B) Einverständniserklärung über die Bereitstellung und Nutzung der Bachelorarbeit / Masterarbeit / Hausarbeit in elektronischer Form zur Überprüfung durch Plagiatssoftware

Eingereichte Arbeiten können mit der Software Plagscan auf einem hauseigenen Server auf Übereinstimmung mit externen Quellen und der institutionseigenen Datenbank untersucht werden. Zum Zweck des Abgleichs mit zukünftig zu überprüfenden Studien- und Prüfungsarbeiten kann die Arbeit dauerhaft in der institutionseigenen Datenbank der Universität Bremen gespeichert werden.

- x Ich bin damit einverstanden, dass die von mir vorgelegte und verfasste Arbeit zum Zweck der Überprüfung auf Plagiate auf den Plagscan-Server der Universität Bremen hochgeladen wird.

- x Ich bin ebenfalls damit einverstanden, dass die von mir vorgelegte und verfasste Arbeit zum o.g. Zweck auf dem Plagscan-Server der Universität Bremen hochgeladen u. dauerhaft auf dem Plagscan-Server gespeichert wird.

Ich bin nicht damit einverstanden, dass die von mir vorgelegte u. verfasste Arbeit zum o.g. Zweck auf dem Plagscan-Server der Universität Bremen hochgeladen u. dauerhaft gespeichert wird.

Mit meiner Unterschrift versichere ich, dass ich die obenstehenden Erklärungen gelesen und verstanden habe. Mit meiner Unterschrift bestätige ich die Richtigkeit der oben gemachten Angaben.

01.12.2022, Bremen, Henric Kuch

Datum, Ort, Unterschrift